© 2016. Published by The Company of Biologists Ltd | Development (2016) 143, 1753-1765 doi:10.1242/dev.131102

RESEARCH ARTICLE

Molecular control of two novel migratory paths for CGE-derived interneurons in the developing mouse brain

Audrey Touzot[1,2,*], Nuria Ruiz-Reig[1,2,3,*], Tania Vitalis[4] and Michèle Studer[1,2,‡]

ABSTRACT

GABAergic interneurons are highly heterogeneous and originate in the subpallium mainly from the medial (MGE) and caudal (CGE) ganglionic eminences according to a precise temporal sequence. MGE-derived cells disperse dorsally and migrate towards all regions of the cortex, but little is known about how CGE-derived cells reach their targets during development. Here, we unravel the existence of two novel CGE caudo-rostral migratory streams, one located laterally (LMS) and the other one more medially (MMS), that, together with the well-known caudal migratory stream (CMS), contribute to populate the neocortex, hippocampus and amygdala. These paths appear in a precise temporal sequence and express a distinct combination of transcription factors, such as SP8, PROX1, COUP-TFI and COUP-TFII. By inactivating COUP-TFI in developing interneurons, the lateral and medial streams are perturbed and expression of SP8 and COUP-TFII affected. As a consequence, adult mutant neocortices have laminar-specific alterations of distinct cortical interneuron subtypes. Overall, we propose that the existence of spatially and temporally regulated migratory paths in the subpallium contributes to the laminar distribution and specification of distinct interneuron subpopulations in the adult brain.

KEY WORDS: COUP-TFI, COUP-TFII, SP8, PROX1, 5HT3aR, Caudal ganglionic eminence, Development, Interneuron migration, Mouse brain

INTRODUCTION

In rodents, different interneuron (IN) subtypes are produced in spatially and temporally distinct regions in the subpallium that consist of the ganglionic eminences (GEs) and preoptic area (POA) domain (Butt et al., 2005; Fogarty et al., 2007; Gelman et al., 2009; Miyoshi et al., 2010; Xu et al., 2004). The medial ganglionic eminence (MGE) represents the major source (~70%) of cortical INs (Anderson et al., 2001; Jiménez et al., 2002; Marín, 2013; Wichterle et al., 2001). The majority of these early-born MGE-derived INs express either parvalbumin (PV; PVALB – Mouse Genome Informatics) or somatostatin (SST) and migrate dorsally to populate deep layers of the neocortex (Valcanis and Tan, 2003; Wichterle et al., 2001; Xu et al., 2004). The caudal ganglionic eminence (CGE) is responsible for producing late-born INs (~30% of all INs) (Miyoshi et al., 2010; Nery et al., 2002; Rudy et al., 2011; Vitalis and Rossier, 2011), which preferentially integrate superficial layers of the neocortex, whereas the POA contributes to a minor pool of cortical INs (Gelman et al., 2009, 2011). The serotonergic ionotropic receptor 5HT3aR (HTR3A – Mouse Genome Informatics) is expressed in the neocortex in all CGE-derived GABAergic INs, such as bipolar calretinin (CR; CALB2 – Mouse Genome Informatics)-, vasoactive intestinal peptide (VIP)-, cholecystokinin (CCK)- and reelin (RLN; RELN – Mouse Genome Informatics)-expressing cells, including multipolar or neurogliaform INs expressing neuropeptide Y (NPY), but not in PV- and SST-positive INs (Murthy et al., 2014; Lee et al., 2010; Vucurovic et al., 2010).

Molecular determinants of the MGE, such as the Dlx homeobox genes *Lhx6*, *Sox6* and *Nkx2.1*, are crucial for the specification and/or migration of the PV- and SST-positive subsets of INs (reviewed by Kessaris et al., 2014; Marín, 2013); however, less is known about the factors and molecular mechanisms controlling the fate determination and migration of CGE-derived cells. The orphan nuclear receptors *COUP-TFI* (also called *Nr2f1*) and *COUP-TFII* (*Nr2f2*) were the first transcriptional regulators found to be enriched in the CGE and required in the migration of GABAergic INs (Tripodi et al., 2004). Whereas COUP-TFII acts mainly in directing CGE-derived cells to the caudal migratory stream (CMS) (Cai et al., 2013; Kanatani et al., 2008; Yozu et al., 2005), COUP-TFI is required for the correct balance between MGE- and CGE-derived INs in the developing neocortex (Lodato et al., 2011b), but its role in migration is less known. *5HT3aR* is expressed in migrating and mature CGE- and POA-derived cells (Lee et al., 2010; Vucurovic et al., 2010) and is cell-autonomously required for the migration and positioning of RLN^+ INs in the neocortex (Murthy et al., 2014). Finally, SP8 and PROX1 are transcription factors expressed principally in subpopulations of lateral ganglionic eminence (LGE)/CGE-derived cortical INs (Ma et al., 2012; Rubin and Kessaris, 2013; Rudy et al., 2011) and a recent report has demonstrated a crucial role for PROX1 in the embryonic and postnatal acquisition of CGE-derived cortical IN properties (Miyoshi et al., 2015).

To reach their final destination, early postmitotic INs start migrating through distinct routes: the MGE-derived cells tangentially migrate dorso-laterally towards the cortex before reaching their final laminar positions by radial migration (reviewed by Guo and Anton, 2014; Marín, 2013), whereas CGE-derived cells seem to colonize the cortex primarily through its caudal pole (Yozu et al., 2005). However, CGE-derived INs are not only dispersed all over the cortex but are also found in various brain regions in the adult, including the hippocampus and amygdala (Chittajallu et al., 2013; Lee et al., 2010; Miyoshi et al., 2010; Nery et al., 2002; Vucurovic et al., 2010; Yozu et al., 2005); how they reach their final positions during development is still unclear (Tanaka and Nakajima, 2012). In addition, apart from COUP-TFII (Kanatani et al., 2008, 2015), the molecular mechanisms controlling

[1]Univ. Nice Sophia Antipolis, INSERM U1091, CNRS UMR7277, iBV, Nice 06100, France. [2]iBV, Institut de Biologie Valrose, Univ. Sophia Antipolis, Bâtiment Sciences Naturelles; UFR Sciences; Parc Valrose, 28, avenue Valrose, Nice Cedex 2 06108, France. [3]Instituto de Neurociencias de Alicante (Consejo Superior de Investigaciones Cientificas-Universidad Miguel Hernandez, CSIC-UMH), Aliante 03550, Spain. [4]Inserm U1141 PROTECT, Hôpital Robert-Debré, Paris 75019, France.
*These authors contributed equally to this work

‡Author for correspondence (michele.studer@unice.fr)

Received 21 September 2015; Accepted 17 March 2016

Development (2016) 143, 1753-1765 doi:10.1242/dev.131102

the tangential migration of CGE-derived cells remain to be elucidated.

In this study, we show that CGE-derived INs use additional paths other than the CMS to reach their final positions. Two novel caudo-rostral streams, one located laterally and the other more medially, allow CGE-derived INs to migrate either dorsally towards the LGE or ventrally towards the POA. PROX1, SP8 and COUP-TF transcription factors are all expressed in these streams with SP8 and COUP-TFII being predominant in the lateral stream, and COUP-TFII in the medial and caudal streams. Inactivation of COUP-TFI affects the rate of SP8^{+} migrating cells in the lateral migratory stream (LMS) and COUP-TFII^{+} cells in the medial migratory stream (MMS), but has no effect on the CMS. The laminar distribution of CGE-derived INs, such as RLN^{+}, single and double VIP^{+}CR^{+} cells, is altered in the somatosensory cortex of adult *COUP-TFI* mutant mice, suggesting that COUP-TFI controls the distribution of CGE-derived INs by regulating SP8 and COUP-TFII expression within their migratory paths. Together, this study reveals the presence of two novel CGE-derived paths involved in populating distinct structures of the brain and contributes to deciphering the molecular mechanisms required in the decision-making steps of interneuron tangential migration.

RESULTS

Identification of two novel tangentially CGE-derived paths in the mouse subpallium

To understand how CGE-derived INs reach their multiple targets, we used the *5HT3aR-GFP* mouse transgenic line, previously reported to label the totality of CGE-derived cortical INs in embryos and in adult mice (Inta et al., 2008; Lee et al., 2010; Murthy et al., 2014; Rudy et al., 2011; Vucurovic et al., 2010). Embryonic day (E) 11.5 to E18.5 *5HT3aR-GFP*$^{+}$ brains were cut in a horizontal plane allowing an overview of all three GE structures in one section (Fig. 1A). In these views, the cortical tissue or pallium is located laterally and the thalamus medially (Fig. 1B). Several sections along the dorso-ventral axis were analysed and the distribution of GFP^{+} cells compared with coronal antero-posterior sections of the same age (Fig. S1).

High levels of GFP are observed in the pallium from E11.5 to E13.5, but these cells are also positive for TBR1 (Fig. S2A-B‴), indicating that they represent glutamatergic preplate and subplate cells (Hevner et al., 2001) transiently expressing *5HT3aR-GFP*. Double RLN^{+}GFP^{+} cells in the marginal zone of E11.5 and E13.5 embryos represent Cajal–Retzius neurons (Fig. S2A-B‴; yellow arrowheads) maintained until postnatal stages, as previously described (Chameau et al., 2009; Engel et al., 2013). At the same time, GFP^{+} cells migrating though the intermediate and marginal zones express the early GABAergic marker calbindin (Fig. S2C-C‴), indicating that at this stage *5HT3aR-GFP*$^{+}$ interneurons invade the cortical plate.

Horizontal and coronal sections show that GFP^{+} cells are detected in the LGE and in some laterally and dorsally migrating cells (unfilled arrowheads in Fig. 1C-E and Fig. S1B-E). As MGE-derived cells do not express *5HT3aR* (Lee et al., 2010; Vucurovic et al., 2010), these cells might either be generated locally and/or derive from the POA (Fig. S1B′-E′, unfilled arrowheads). Notably, E11.5 horizontal sections at ventral levels also reveal a stream of

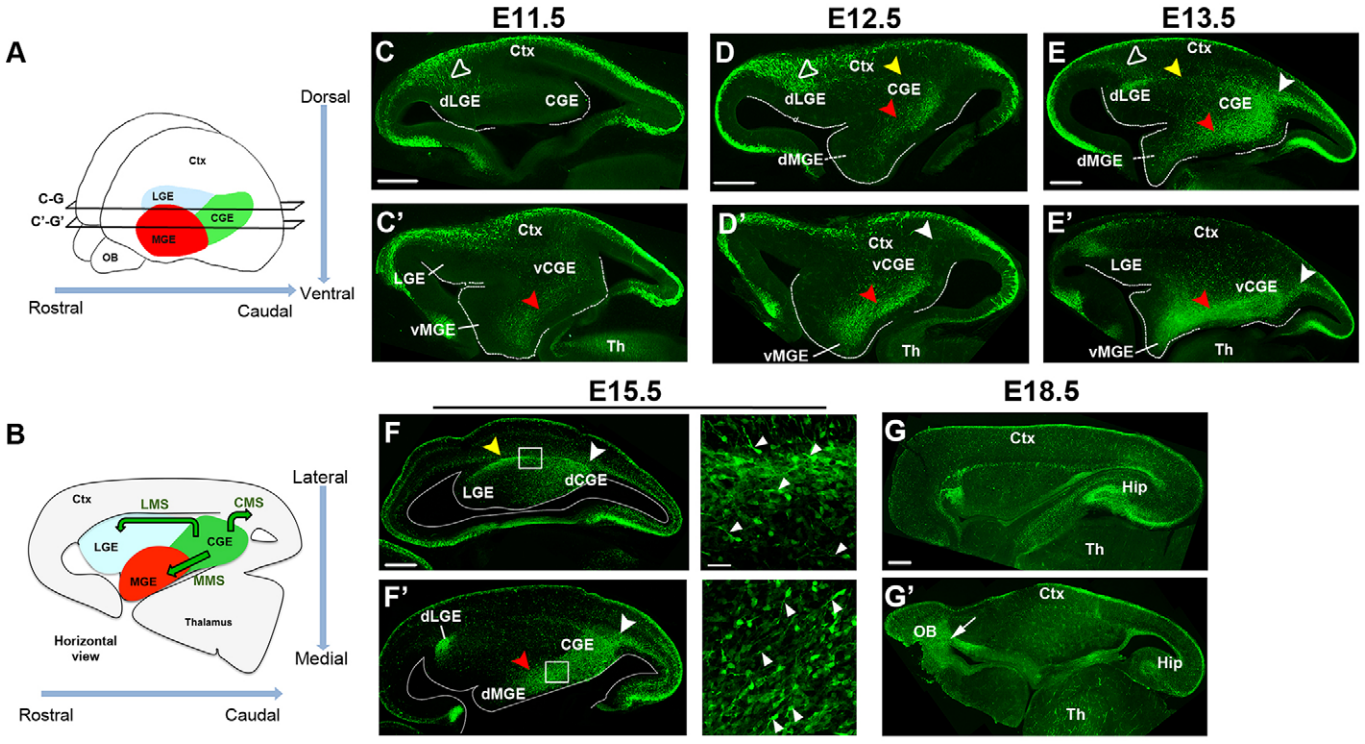

Fig. 1. Temporal sequence of the different 5HT3aR-GFP^{+} migratory streams in the developing mouse. (A) Schematic of an embryological mouse brain indicating the plane of horizontal sections shown in C-G′. (B) Schematic of a horizontal E13.5 brain indicating the caudal, medial and lateral ganglionic eminences. Green arrows highlight the three migratory streams described in the text. (C-G′) Horizontal sections of *5HT3aR-GFP* embryos immunostained with GFP at the stages indicated above. Red arrowheads point to the MMS, yellow arrowheads to the LMS, and white arrowheads to the CMS. Unfilled arrowheads indicate GFP^{+} cells migrating from the dLGE. White arrows point to cells migrating rostrally to the olfactory bulb. Ctx, cortex; dCGE, dorsal caudal ganglionic eminence; dLGE, dorsal lateral ganglionic eminence; dMGE, dorsal medial ganglionic eminence; vCGE, ventral caudal ganglionic eminence; vMGE, ventral medial ganglionic eminence; Hip, hippocampus; OB, olfactory bulb; Th, thalamus. Scale bars: 300 µm.

Development (2016) 143, 1753-1765 doi:10.1242/dev.131102

GFP$^+$ cells between the CGE and MGE (Fig. 1C′, red arrowhead), which increases in intensity at E12.5 and E13.5 (Fig. 1D′,E′). In addition, a few GFP$^+$ cells lateral and caudal to the CGE appear at E12.5 (Fig. 1D,D′, yellow and white arrowheads, respectively), and will form two prominent streams at E13.5, one migrating caudo-dorsally (Fig. 1E,E′; Fig. S1B″-E″) and previously described as the CMS (Yozu et al., 2005), and another one laterally between the CGE and LGE (Fig. 1E, yellow arrowheads), here termed the LMS. The other path between the CGE and MGE becomes very prominent at E13.5 (Fig. 1E,E′, red arrowheads) and is referred to as the MMS throughout this study. Thus, *5HT3aR-GFP*$^+$ cells seem to undertake a lateral, medial and/or caudal path before reaching the cortex by dorsal migration.

All the streams attain their highest intensity at E15.5 (Fig. 1F,F′; Fig. S1E-E″) in accordance with the peak of CGE cell production (Miyoshi et al., 2010), and leading processes in the dorsal LMS and ventral MMS are oriented rostrally (Fig. 1F,F′, white arrowheads in high magnification views) in line with a caudal-to-rostral migration. At E18.5, *5HT3aR-GFP*$^+$ cells have reached the neocortex, hippocampus and amygdala (Fig. 1G,G′; Fig. S1F-F″) and the olfactory bulb through the rostral migratory stream (RMS) (Fig. 1G′, arrow), as previously described (Inta et al., 2008). Taken together, our time course on horizontal and coronal sections of the *5HT3aR-GFP* mouse line revealed two CGE-derived additional migratory paths besides the caudal one (Fig. 1B) in the subpallium of E11.5 to E15.5 embryos.

Caudo-rostral tangential migration of CGE-derived cells in the mouse subpallium

To confirm a caudo-rostral migratory direction of *5HT3aR-GFP*$^+$ cells in the LMS and MMS, the CGE of an E13.5 *5HT3aR-GFP* embryo was homotopically grafted into a non-GFP littermate, and horizontal organotypic slices were incubated for 2 days *in vitro* (DIV) (Fig. 2A). GFP$^+$ cells migrating away from the grafted site take several paths, including the lateral, medial and caudal ones (Fig. 2B-B‴). Direction of their leading processes confirmed a caudal-to-rostral type of migration (Fig. 2A; Fig. 2B′-B‴, red arrows). To confirm CGE-derived caudo-rostral migration, we injected the lipophilic tracer DiI or introduced the cell tracker CMTPX loaded on resin beads into the CGE of E14.5 *5HT3aR-GFP* horizontal organotypic slices (Fig. S3A). Upon internalization by the cells, the fluorescent DiI will be retained and the CMTPX will be converted to a fluorescent compound (Haugland, 2002). Brain slices were then analysed for the presence of the tracer and expression of GFP in the different streams (Fig. S3B). DiI- and CMTPX-traced cells were found in several GFP$^+$ cells in the CMS, LMS and MMS (Fig. S3C-E″ for DiI; Fig. S3F-L′ for CMTPX), but not in cells expressing NKX2.1, a marker for the MGE/POA (Sussel et al., 1999; Xu et al., 2008) (Fig. S3K-N′). This indicates that GFP$^+$ cells migrating towards the MGE do originate from the CGE and not from the POA. Taken together, our three independent tracing approaches confirm that 5HT3aR-GFP$^+$/CGE-derived cells migrate caudo-rostrally from the CGE to the LGE through the LMS and from the CGE to the MGE through the MMS (Fig. 2A; Fig. S3A).

Expression of transcription factors in the CGE-migrating streams

Next, we assessed whether the different migrating populations express a unique transcription factor or a combination of CGE-specific transcription factors (Fig. 3). COUP-TF nuclear receptors are preferentially restricted to the CGE from E13.5 and maintained in CGE-derived cortical INs (Cai et al., 2013; Kanatani et al., 2008; Lodato et al., 2011b; Tripodi et al., 2004). The transcription factor SP8 is expressed in CGE-derived cortical INs and in dorsal LGE (dLGE)-derived olfactory bulb INs (Ma et al., 2012), whereas PROX1 is highly expressed in CGE-derived cortical INs and in a subpopulation of POA-derived INs (Rubin and Kessaris, 2013; Miyoshi et al., 2015).

COUP-TFI and/or COUP-TFII proteins are localized in different proportions within the GFP$^+$ migrating streams at E15.5 with a high representation of single COUP-TFII-expressing cells in the LMS (41%) compared with 24% in the MMS (Fig. 3A-D). In the CMS, 29% of GFP$^+$ cells express only COUP-TFII and 14% are positive for both COUP-TFI and COUP-TFII (Fig. 3D), revealing that the CMS has the greatest proportion of double COUP-TF-expressing cells compared with the other migrating streams. By contrast, SP8 and/or PROX1 are detected at a much lower level in the CMS and

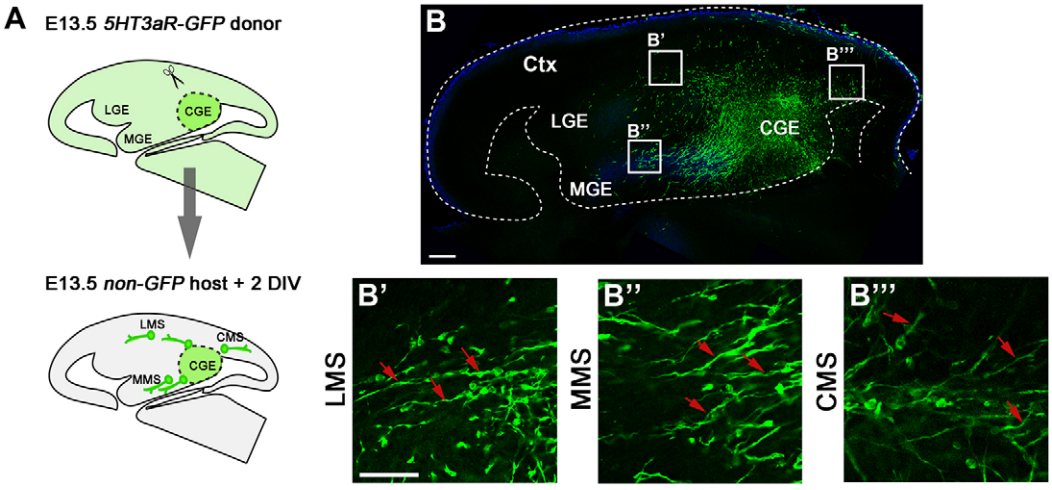

Fig. 2. CGE-derived 5HT3aR-GFP$^+$ cells migrate rostrally and caudally. (A) Schematic of the experimental approach in which the CGE is cut from a E13.5 *5HT3aR-GFP* horizontal organotypic brain section and homotopically grafted into a non-GFP section of the same age and cultured for 2 DIV. Cells exiting from the graft are drawn with their leading process to indicate the direction of migration. (B) Whole view of the grafted horizontal section shows spreading of GFP$^+$ cells into rostral and caudal directions. (B′-B‴) High magnification views of boxes in B indicate the leading processes of migrating GFP$^+$ grafted cells (red arrows). Ctx, cortex. Scale bars: 300 µm (B); 50 µm (B′-B‴).

Development (2016) 143, 1753-1765 doi:10.1242/dev.131102

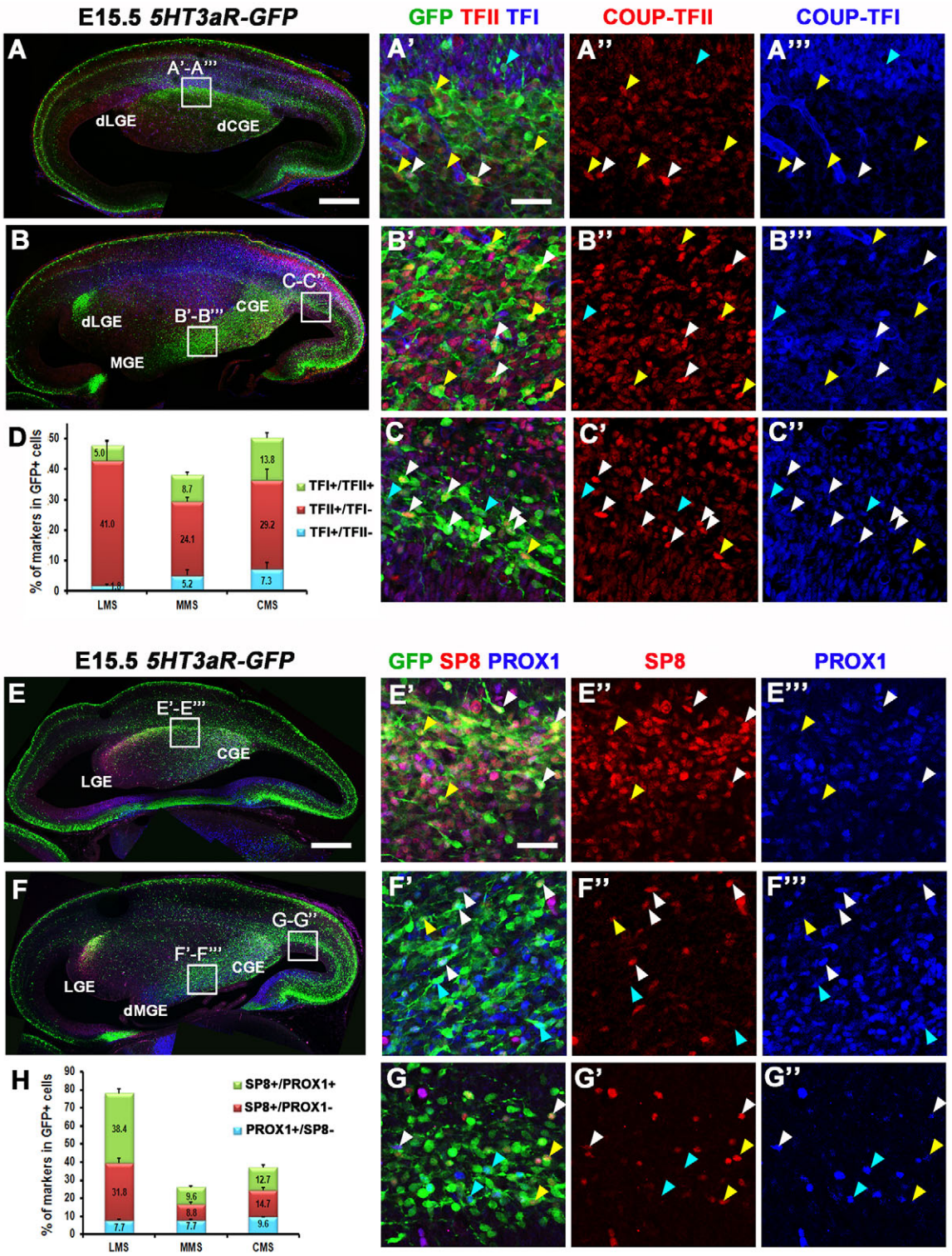

Fig. 3. Transcription factors expressed along the streams in the subpallium of *5HT3aR-GFP* embryos. (A-D) Triple IF of dorsal (A) and ventral (B) horizontal sections of E15.5 *5HT3aR-GFP* brains stained with COUP-TFI and COUP-TFII. (A′-C″) High magnification views of details depicted in the boxes in A,B. White arrowheads indicate triple-labelled cells; yellow and blue arrowheads point to double-positive cells. (D) Percentage of single- and double-labelled COUP-TF^{+} cells expressing GFP in the different streams. (E-H) Triple IF of dorsal (E) and ventral (F) horizontal sections of E15.5 *5HT3aR-GFP* brains stained with SP8 and PROX1. (E′-G″) High magnification views of the boxes in E,F. White arrowheads indicate triple-labelled cells; yellow and blue arrowheads point to double-positive cells. (H) Percentage of single and double SP8^{+} and PROX1^{+} cells expressing GFP in the different streams. Error bars indicate s.e.m. dCGE, dorsal caudal ganglionic eminence; dLGE, dorsal lateral ganglionic eminence; dMGE, dorsal medial ganglionic eminence. Scale bars: 300 µm (A,B,E,F); 25 µm (A′-G″).

MMS, and are instead highly represented in the LMS, with 70% of GFP^{+} cells expressing SP8, 46% PROX1, and 38% both SP8 and PROX1 (Fig. 3E-H). Thus, whereas COUP-TF members are well expressed in all three streams, SP8^{+} and double SP8^{+}PROX1^{+} cells are preferentially located in the lateral path (LMS) during the peak of CGE-derived IN production.

Development (2016) 143, 1753-1765 doi:10.1242/dev.131102

Previous studies have shown that SP8 is also expressed in the dLGE, which will give rise to INs of the olfactory bulb and amygdala (Jiang et al., 2013; Li et al., 2011; Ma et al., 2012; Stenman et al., 2003; Waclaw et al., 2006, 2010). To distinguish between the two sources of SP8$^+$ cells migrating either ventrally or dorsally, we labelled SP8$^+$GFP$^+$ cells with ER81 (ETV1 – Mouse Genome Informatics), a transcription factor specific for olfactory bulb-derived INs (Stenman et al., 2003), on E15.5 coronal sections and in the adult olfactory bulb (Fig. S4). Triple-positive cells are only found in the dLGE at rostralmost levels (Fig. S4A-A‴) and in the granule layer of adult olfactory bulbs (Fig. S4E-E‴). No GFP$^+$ cells within the LMS express ER81 (Fig. S4B-D‴), and double SP8$^+$GFP$^+$ cells are observed migrating dorsally towards the cortex (Fig. S4B′-D′, white arrowheads). These data imply that SP8$^+$ cells might originate from a local dLGE source and migrate towards the olfactory bulb, but also derive from the CGE and migrate dorso-laterally along the LMS before reaching the cortex.

High contribution of CGE-derived PROX1$^+$GFP$^+$ cells to the cortex, hippocampus and amygdala of juvenile brains

Next, we estimated the contribution of CGE-derived *5HT3aR-GFP*$^+$ cells expressing PROX1 and/or SP8 in juvenile brains by homochronically grafting CGE-derived neurons from E14.5 *5HT3aR-GFP* embryos into wild-type host embryos (Fig. 4A) (Vucurovic et al., 2010). The distribution of GFP$^+$/CGE-grafted cells was subsequently analysed in the somatosensory cortex, hippocampus and amygdala of postnatal day (P) 21 host brains (Fig. 4B). The majority of grafted cells (85%) populated several amygdaloid nuclei, whereas 9% and 6% were localized in the cortex and hippocampus, respectively (Fig. 4B). We then investigated the proportions of GFP$^+$ cells expressing either SP8 or PROX1, or both, in P21 grafted brains (Fig. 4C). Notably, 56% of 947 *5HT3aR-GFP*$^+$ integrated cells express PROX1 and 39% SP8 in the cortex, of which almost 30% were double positive. Single PROX1$^+$ cells were well represented in the hippocampus and amygdala compared with single SP8- and double-expressing cells (Fig. 4D). Thus, our data show that a high proportion of CGE-derived cells at E14.5 reach amygdalar structures, and that within these transplanted GFP$^+$ cells the majority express PROX1.

Subtype characterization and layer distribution of CGE-derived pallial SP8- and PROX1-expressing INs in adult *5HT3aR-GFP* mice

Our graft experiments illustrate the contribution of PROX1- and/or SP8-expressing CGE-derived cells in different brain structures at a unique time point; however, CGE cells start to migrate from E11.5 (Fig. 1; Fig. S1). Thus, to have an overview of all *5HT3aR-GFP*$^+$ cells expressing SP8, PROX1 and/or COUP-TFII in adult brains, we first analysed the percentage and laminar distribution of single and/or double SP8- and PROX1-expressing GFP$^+$ INs in the somatosensory cortex of 2-month-old *5HT3aR-GFP* mice (Fig. 5). We found that the majority (57%) of GFP$^+$ cortical INs is double positive for SP8 and PROX1, whereas single PROX1$^+$ (SP8$^-$) and single SP8$^+$ (PROX1$^-$) cells account for 27% and <5%, respectively, of all GFP$^+$ cortical INs (Fig. 5A-C,K). The different subpopulations are distributed fairly evenly in all layers, although the double-expressing cells tend to be located in deeper layers and the single-expressing cells in upper layers (Fig. 5L). This indicates that in the somatosensory cortex 84% of all *5HT3aR-GFP*$^+$ cells express PROX1, of which more than half are double positive for SP8.

Next, we investigated the proportion of *5HT3aR-GFP*$^+$ cells expressing PROX1, SP8 and/or COUP-TFII together with particular cortical IN subtype markers, such as RLN, VIP and CR, in the adult somatosensory cortex (Fig. 5D-J) (Rudy et al., 2011; Vucurovic et al., 2010). The populations of SP8- or PROX1-expressing cells colocalize with VIP and RLN in roughly equal proportions (24% and 26%, respectively, for SP8; 23% and 20% for PROX1) (Fig. 5D,E,H,I,M), but are co-expressed with CR in only 13% of GFP$^+$ INs, whereas double COUP-TFII$^+$RLN$^+$ represent 18% of all *5HT3aR-GFP*$^+$ in the cortex (Fig. 5F,G,J,M). Regarding the laminar distribution, we found that within the PROX1$^+$GFP$^+$ cell population, layer IV includes a higher percentage of CR$^+$ than RLN$^+$ and VIP$^+$ cells, which are instead more represented in layers I-III and VI (Fig. 5N). By contrast, within the SP8$^+$GFP$^+$ population, layer V has the highest percentage of VIP$^+$ and the lowest preference of CR$^+$, whereas the RLN$^+$ population is almost evenly distributed in all layers (Fig. 5N). Together, CGE-derived *5HT3aR-GFP*$^+$ cells expressing PROX1, SP8 or COUP-TFII are distributed along the whole radial extend of the cortex and consist mainly of RLN- or VIP-positive INs.

Moreover, 55% and 53% of GFP$^+$ cells express PROX1 in the basolateral (BLA) and medial amygdala (MeA), respectively (Fig. S5A-B‴,D), compared with a minor SP8$^+$ or double PROX1$^+$SP8$^+$ population (Fig. S5D). Finally, 38% express PROX1$^+$ and 21% express SP8$^+$ within the GFP$^+$ cells located in the hippocampus, (Fig. S5C-D). Thus, PROX1 is highly expressed not only in the CGE-derived cells reaching the neocortex, as previously described (Miyoshi et al., 2015), but also in the *5HT3aR-GFP*$^+$ cells migrating to the amygdaloid complex and the hippocampus.

The CGE-derived migratory streams are affected in the absence of COUP-TFI

Next, we assessed whether transcription factors expressed in the caudo-rostral streams might be directly involved in the migration and specification of CGE-derived cortical INs. Because *Sp8* conditional mice fail to show any evident interneuronal defects (Ma et al., 2012) and *Prox1* conditional mice became available only very recently (Miyoshi et al., 2015), we took advantage of our previously generated *COUP-TFI* conditional knockout (CKO) mouse line (Lodato et al., 2011b), in which the *COUP-TFI$^{flox/flox}$* mouse is crossed to the *Dlx5/6-Cre* line to generate *COUP-TFI::Dlx5/6-Cre* (hereafter called TFICKO). We previously showed that absence of COUP-TFI leads to an increase of MGE-derived PV$^+$ INs and resistance to GABA-dependent pharmacologically induced seizures (Lodato et al., 2011b). However, COUP-TFI gets restricted to the CGE from E13 onwards and its expression is maintained in CGE-derived IN subtypes (Lodato et al., 2011b). To assess its specific action on CGE-derived cortical IN specification and migration, we crossed the TFICKO mouse to the *5HT3aR-GFP* reporter line and followed the migration and molecular specification of CGE-derived paths in horizontal sections (Fig. 6). At E13.5, when the MMS and CMS are well established, the density of postmitotic GFP$^+$ cells in these two streams is decreased in TFICKO brains (compare Fig. 6A,A″,A‴ with B,B″,B‴, respectively), whereas the few cells located in the LMS and LGE are not altered (Fig. 6A′,B′). By contrast, at E15.5, during the peak of CGE production, the number of GFP$^+$ cells increases by ∼50% in the LMS (Fig. 6C,C′,D,D′, E; TFICKO 154.0±23.7% versus control 100%; n=3; P=0.042) and by almost 25% in the mutant versus the control in the MMS (Fig. 6C″,D″) (Fig. 6E; TFICKO 123.8±9.9% versus control 100%; n=3; P=0.026). No statistical difference was detected in the amount of caudally migrating GFP$^+$ cells (Fig. 6E, CMS).

Development (2016) 143, 1753-1765 doi:10.1242/dev.131102

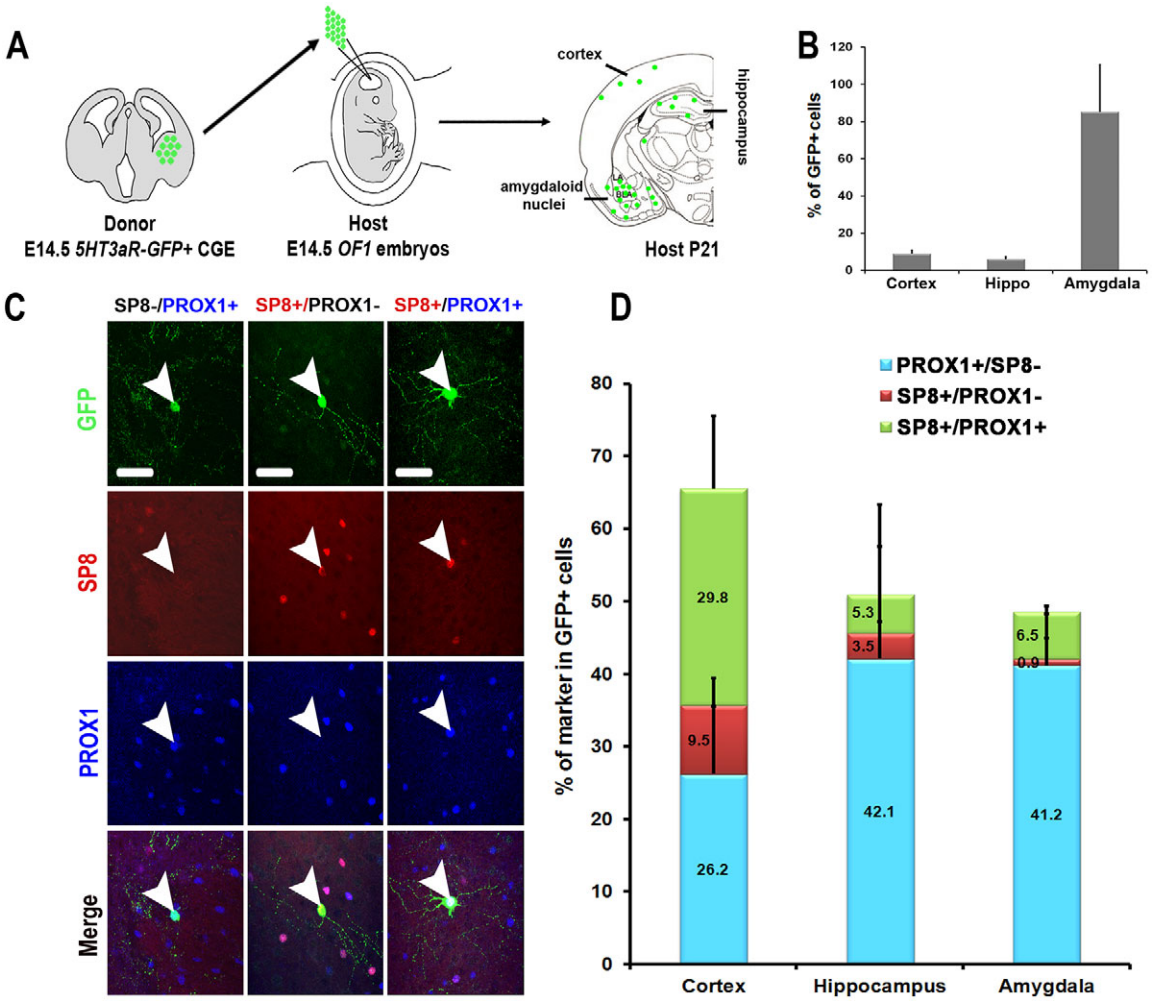

Fig. 4. Anatomical and molecular fate of the *in utero*-grafted CGE-5HT3aR-GFP$^+$ cells in juvenile brains. (A) Schematic illustrating the *in utero* grafting strategy from a GFP-positive donor (green cells) to a GFP-negative host and the localization of GFP$^+$ cells in the somatosensory cortex, hippocampus and amygdala of P21-grafted brains. (B) Distribution of GFP$^+$ cells in the grafted brains. (C) Representative examples of GFP-grafted cells stained with PROX1 and SP8. Arrowheads indicate double- or triple-positive grafted cells. (D) Histogram showing the percentage of grafted cells positive for PROX1 and/or SP8 in the different brain structures. Error bars indicate s.e.m. Scale bars: 50 µm.

We hypothesized that loss of COUP-TFI would affect cell proliferation in the CGE at E13.5 resulting in a reduction of CGE-derived GFP$^+$ migrating cells. Indeed, more proliferating cells are detected in the subventricular (SVZ) but not ventricular (VZ) zone of mutant embryos (Fig. 6F-H; TFICKO 146.3±9.2% versus control 100%; n=3; P=0.065), in accordance with the selective inactivation of *COUP-TFI* in the SVZ (Lodato et al., 2011b). This implies that CGE precursors initially proliferate more and accumulate in the SVZ before being released at E15.5 and allowed to migrate along the LMS and MMS, as observed in Fig. 6D. Thus, COUP-TFI both controls the rate of proliferating cells in the SVZ and promotes CGE migrating cells to take a caudo-rostral direction.

COUP-TFI regulates SP8 expression along the lateral stream and COUP-TFII along the medial stream

We next assessed whether COUP-TFI controls the expression of SP8, PROX1 and/or COUP-TFII along the different CGE-derived GFP$^+$ migratory streams described in this study (Fig. 1B). E15.5 horizontal *5HT3aR-GFP* sections were immunostained with SP8, PROX1 or COUP-TFII antibodies (Fig. 7A-I′) and the density of cells double positive for GFP and one of these markers was evaluated in the LMS, MMS and CMS (Fig. 7J). The number of GFP$^+$SP8$^+$ cells was increased twofold in the LMS of *COUP-TFI* mutants (Fig. 7A,A′,J; TFICKO 152.7±33.0 cells versus control 74.4±4.0 cells; n=6; P=0.019), whereas no differences were found in the PROX1$^+$ and COUP-TFII$^+$ GFP-expressing populations (Fig. 7B-C′,J). By contrast, only the COUP-TFII$^+$GFP$^+$ population was significantly increased in the MMS of *COUP-TFI* mutants (Fig. 7F,F′,J; TFICKO 53.1±4.9 cells versus control 34.7±6.0; n=6; P=0.045), and not the PROX1$^+$ and SP8$^+$ subpopulations (Fig. 7D-E′,J). As expected from the data shown in Fig. 6E, no changes in the number of GFP$^+$ cells expressing SP8, PROX1 or COUP-TFII were observed in the CMS (Fig. 7G-I′,J). Together, these data indicate that COUP-TFI normally restricts the number of CGE cells taking the lateral path towards the LGE by modulating SP8 expression and the medial path towards the MGE by controlling COUP-TFII.

Loss of COUP-TFI affects RLN- and double VIP/CR-expressing interneurons in the adult somatosensory cortex

The different paths undertaken by CGE-derived neurons might be correlated with specific cortical IN subtypes in the adult cortex. To test this hypothesis, we first evaluated the percentage of the different subtypes of CGE-specific INs in control and *COUP-TFI*

Development (2016) 143, 1753-1765 doi:10.1242/dev.131102

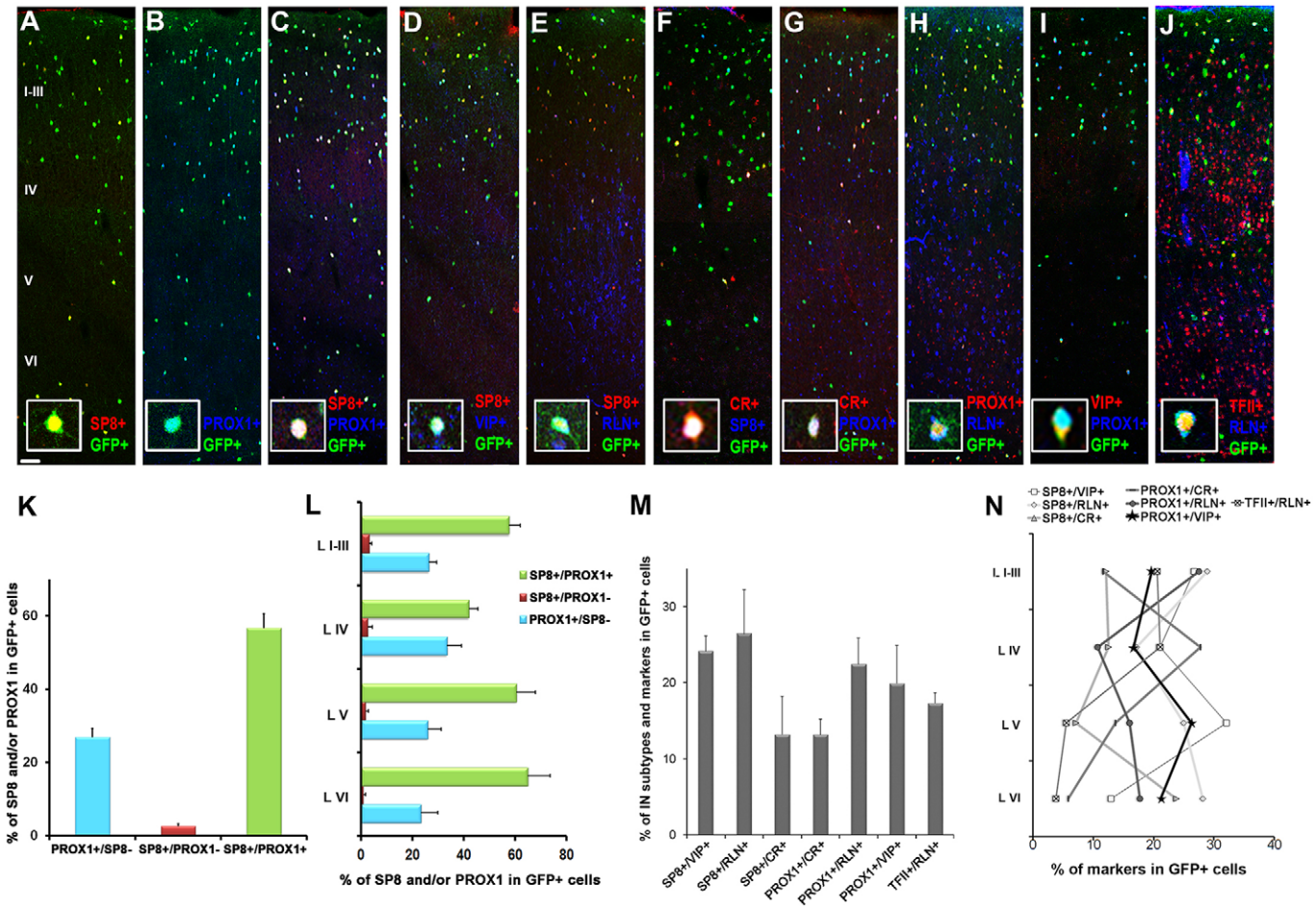

Fig. 5. Molecular characterization and laminar distribution of 5HT3aR-GFP$^+$ in the adult somatosensory cortex. (A-J) Double and triple IF on coronal sections of 2-month-old *5HT3aR-GFP*$^+$ somatosensory cortices with the antibodies indicated. Roman numerals illustrate the location of the different layers. Insets show representative double (A,B)- or triple (C-J)-positive cells. (K) Histogram showing the percentage (±s.e.m.) of single and double SP8$^+$ and/or PROX1$^+$ cells among GFP$^+$ cells. (L) Graph depicting the laminar distribution of single and double SP8$^+$ and/or PROX1$^+$ cells among GFP$^+$ cells. (M) Histogram showing the percentage (±s.e.m.) of cells expressing SP8, PROX1 or COUP-TFII and IN neurochemical markers among GFP$^+$ cells. (N) Graph illustrating the laminar distribution of these populations. Scale bar: 100 µm.

mutant adult somatosensory cortices, and subsequently the same subtypes expressing PROX1, SP8 or COUP-TFII within the *5HT3aR-GFP*$^+$ cell populations (Fig. 8A,A′; compare Fig. 5C-J for controls with Fig. 8B-I for TFICKOs). Overall, we observed that the total number of *5HT3aR-GFP*$^+$ cells is not drastically different in control and adult *COUP-TFI* CKO mice, even if mutants tend to have a slightly higher number of CGE-derived GFP$^+$ INs in the somatosensory cortex (Fig. 8J). Notably, among the CGE-derived GFP$^+$ cell populations, the RLN$^+$ population of cells increased from 27.3±2.1% to 37.1±1.6% (n=3; P=0.002) in adult TFICKO cortices, particularly in layers II-IV and VI (Fig. 8K,L), whereas the small number of double RLN$^+$SST$^+$ cells remained the same within the GFP$^+$ population (data not shown) (Lee et al., 2010), indicating that it is mainly the RLN$^+$ population, comprising neurogliaform cells (Miyoshi et al., 2010), that is affected in the absence of COUP-TFI. Notably, although the single CR- and VIP-expressing populations are only slightly increased (Fig. 8K), the double CR/VIP-expressing GFP$^+$ subpopulation is statistically larger in TFICKO cortices (Fig. 8A,A′,M,N; TFICKO 12.4±1.5% versus control 8.0±1.4%; n=3; P=0.035), particularly in layers IV and V (Fig. 8M).

To further evaluate whether the IN subpopulations affected in the mutants are associated with a particular transcriptional code, we quantified the percentage of *5HT3aR-GFP*$^+$ subtype IN populations expressing either SP8, PROX1 or COUP-TFII and reported their laminar distribution (Fig. 8N-P). No drastic effects were detected in the GFP$^+$ population expressing SP8, PROX1 or COUP-TFII or even double SP8$^+$PROX1$^+$ in adult TFICKO brains (Fig. 8K,N). Similarly, the overall percentage of VIP$^+$, RLN$^+$ or CR$^+$ populations expressing SP8, PROX1 or COUP-TFII was not altered within the GFP$^+$ mutant populations (Fig. 8N). However, we found that the VIP$^+$ subpopulation expressing SP8 is statistically increased, whereas the double PROX1$^+$CR$^+$ subgroup is decreased, in layer VI of *COUP-TFI* CKO brains (Fig. 8O,P). No laminar differences were found in the SP8/RLN-, PROX1/RLN- and COUP-TFII/RLN-expressing populations (data not shown), indicating that the increased RLN population observed in the absence of COUP-TFI is independent of these transcription factors. Thus, COUP-TFI normally modulates the number of RLN$^+$ and double CR$^+$VIP$^+$ CGE-derived cortical INs, and controls the balance between SP8/VIP- and PROX1/CR-expressing cells in layer VI.

DISCUSSION

Previous reports showed that cells located in the CGE can reach several telencephalic regions, such as the cerebral cortex, the hippocampus and the amygdala (Nery et al., 2002; Lee et al., 2010;

Development (2016) 143, 1753-1765 doi:10.1242/dev.131102

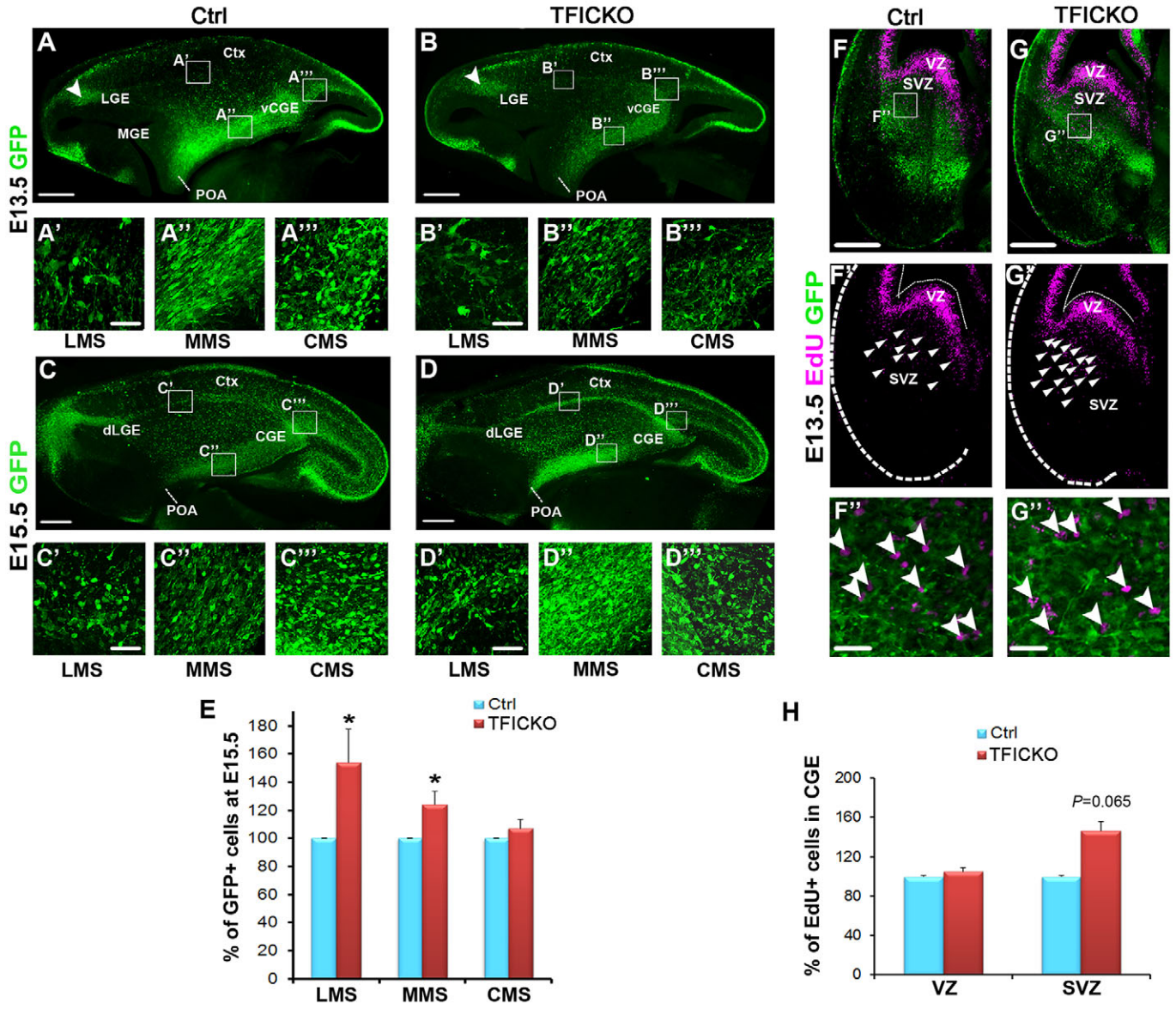

Fig. 6. Altered number of 5HT3aR-GFP$^+$ cells in the migrating streams of *COUP-TFI* mutant embryos. (A-D‴) Horizontal sections (A-D) of *5HT3aR-GFP*$^+$ embryos in control (Ctrl) and *COUP-TFI* mutant (TFICKO) mice. Below, high magnifications of the boxed areas show details of the various streams (A′-D‴). Arrowheads in A,B indicate GFP$^+$ cells in the dLGE at E13.5. (E) Histogram showing the percentage (±s.e.m.) of GFP$^+$ cells in the various streams in Ctrl and *COUP-TFI* mutant embryos. (F-G″) Coronal sections of caudal E13.5 *5HT3aR-GFP*$^+$ embryos after a short EdU pulse (magenta) in control and *COUP-TFI* mutant embryos (F,G). (F′,G′) Arrowheads point to proliferating EdU$^+$ cells in the subventricular zone (SVZ). (F″,G″) Arrowheads indicate no colocalization of EdU and GFP in the SVZ. (H) Histogram depicting the percentage of EdU$^+$ cells in the ventricular (VZ) and SVZ of control and mutant CGE. Data are represented as mean±s.e.m. *$P \leq 0.05$. Note that the P -value is close to significance in the SVZ. dLGE, dorsal lateral ganglionic eminence; vCGE, ventral caudal ganglionic eminence. Scale bars: 300 µm (A-D,F-G′); 50 µm (A′-D‴,F″,G″).

Vucurovic et al., 2010; Yozu et al., 2005), but little was known about how CGE-derived INs were sorted to reach these final targets. In this study, we provide novel evidence that CGE-derived mouse INs disperse from the CGE using distinct migratory paths in the subpallium before reaching their final locations. We also show that several transcriptional regulators required in IN specification and expressed at high levels in the CGE are represented at different ratios within the subpallial streams. Perturbation of one of these transcriptional regulators, COUP-TFI, affects the two caudo-rostral streams and the laminar distribution of distinct CGE-derived IN subtypes. Thus, our study contributes to our understanding of the complex migratory patterns of CGE-derived INs during development.

The existence of two caudo-rostral migratory paths and their contribution

Why do CGE-derived INs need to use so many streams to reach their final targets? We propose at least two main reasons based on our data and other studies. First, because the CGE not only produces INs migrating to the cortex (including piriform and enthorinal cortex), but also to the hippocampus and amygdala (our study; Nery et al., 2002; Vucurovic et al., 2010), we propose that CGE-derived cells take distinct tangential routes to reach their specific targets (Fig. 9). This is already substantiated by the CMS, which directs CGE cells to more caudal brain structures, such as the hippocampus (Chittajallu et al., 2013; Yozu et al., 2005). Here, we propose that the MMS populates the amygdala, as already suggested by short-

Development (2016) 143, 1753-1765 doi:10.1242/dev.131102

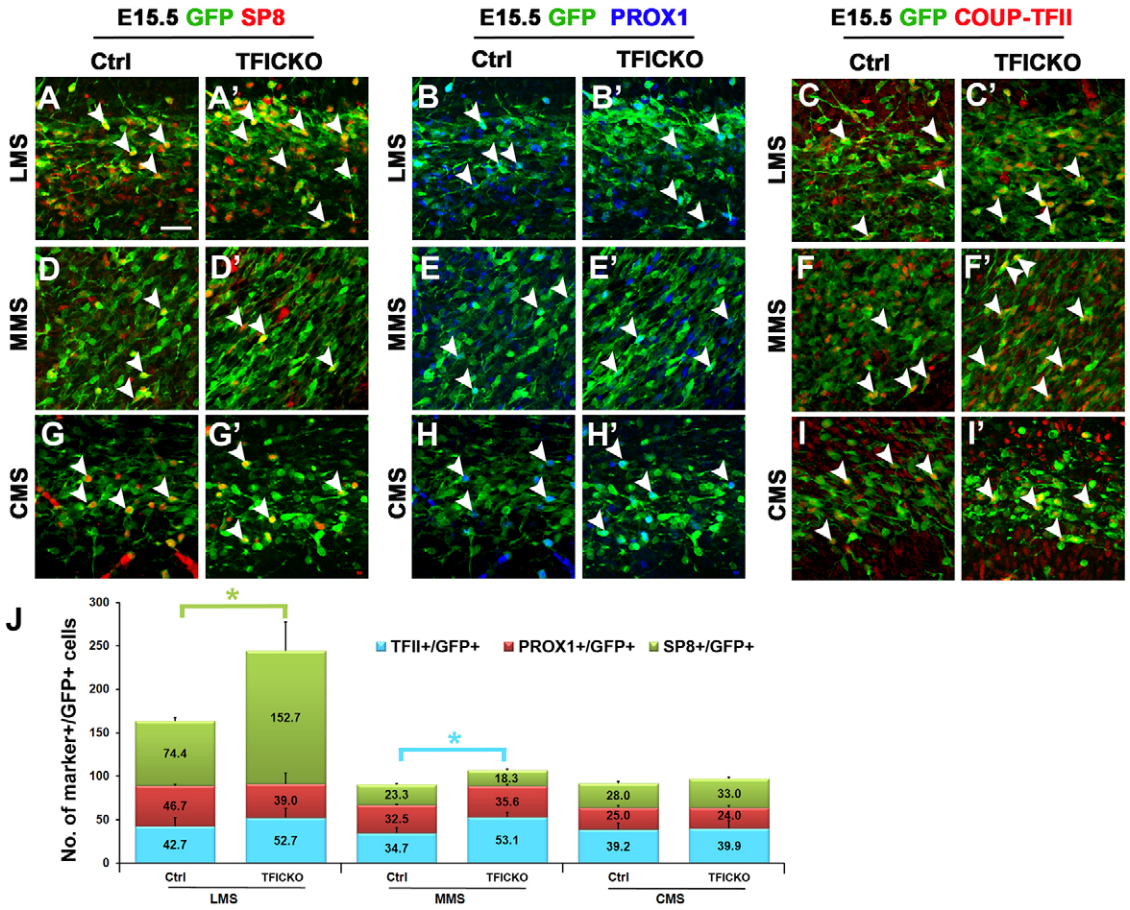

Fig. 7. Altered number of SP8- and COUP-TFII-expressing cells in the migrating streams of *COUP-TFI* mutant *5HT3aR-GFP* embryos. (A-I′) Details of the GFP$^+$ lateral (LMS), medial (MMS) and caudal (CMS) streams immunostained with SP8, PROX1 and COUP-TFII on E15.5 control (Ctrl) and *COUP-TFI* mutant (*TFICKO*) horizontal sections. Arrowheads point to double-expressing cells. (J) Histogram illustrating the density of cells double positive for the markers and for GFP in the different streams. Data are represented as mean±s.e.m. *P≤0.05 (colour-coded according to the marker to which it refers). Scale bar: 25 µm.

term *in vitro* grafts (Vucurovic et al., 2010) and now supported by this study: (1) the majority of E14.5 CGE-grafted cells populate the amygdala in juvenile brains; (2) the massive cohort of GFP$^+$ cells migrating medially is abundant at E12/E13, a stage when CGE-derived cortical INs normally represent only a small fraction (Lee et al., 2010; Miyoshi et al., 2010; Nery et al., 2002; Vucurovic et al., 2010); and (3) the MMS is highly represented by cells expressing COUP-TFII, which plays a relevant role in amygdala patterning (Tang et al., 2012) and which drives POA-derived cells to the medial amygdala (Kanatani et al., 2015).

The second reason why so many paths depart from the CGE might be a temporal one. It is known that CGE/late-migrating INs, in contrast to MGE/early-migrating INs, which populate the cortex in an inside-out mode by temporally matching the integration of projection neurons, colonize the cortex independently of their birthdate (Miyoshi et al., 2007, 2010). The use of spatially and temporally regulated paths might thus allow CGE-derived INs a sequential integration into their correct laminar locations. Indeed, the different paths arise and have their peaks at distinct ages: the MMS is the earliest to start (at E11.5), followed by the LMS at E12.5 and the CMS around E13. The distinct paths might also help in sorting MGE- versus CGE-derived cells with identical birthdate, as radial distribution during cortical plate invasion occurs several days later in CGE-derived populations than in those derived from the MGE (Miyoshi and Fishell, 2011). Hence, we propose that the laminar distribution of distinct cortical IN lineages might be also controlled in the subpallium through individual tangential routes, and not only at the cortical plate level, as previously suggested (Lodato et al., 2011a; Miyoshi and Fishell, 2011).

The lateral stream is highly populated by SP8- and/or PROX1-expressing interneurons

In contrast to the MMS, the LMS might contribute to populating the cerebral cortex, in line with its presence during the peak of CGE-derived cortical IN invasion (Lee et al., 2010; Miyoshi et al., 2010, 2015; Vucurovic et al., 2010). SP8 and/or PROX1 are expressed at high levels in the CGE and maintained in the LMS towards the dLGE, and a conspicuous amount of double SP8$^+$PROX1$^+$ cells are found in GFP$^+$ cells of the cortex expressing typical CGE-derived IN subtype markers, such as VIP, RLN and CR. This suggests that the majority of PROX1$^+$ cortical INs described recently (Miyoshi et al., 2015) might co-express SP8 and that single and double SP8/PROX1-expressing INs might have different properties and functions in the brain. Indeed, PROX1$^+$ cells deriving from the CGE also contribute to the hippocampus and amygdala by using either the streams described in this study or other not yet identified paths. In addition, SP8$^+$ cells are also found in the dLGE before the arrival of LMS cells (this study; Ma et al., 2012), suggesting that the dLGE and CGE represent two independent sources of SP8$^+$ INs. Thus, whereas double SP8$^+$ER81$^+$ cells in the dLGE contribute to olfactory bulb

Development (2016) 143, 1753-1765 doi:10.1242/dev.131102

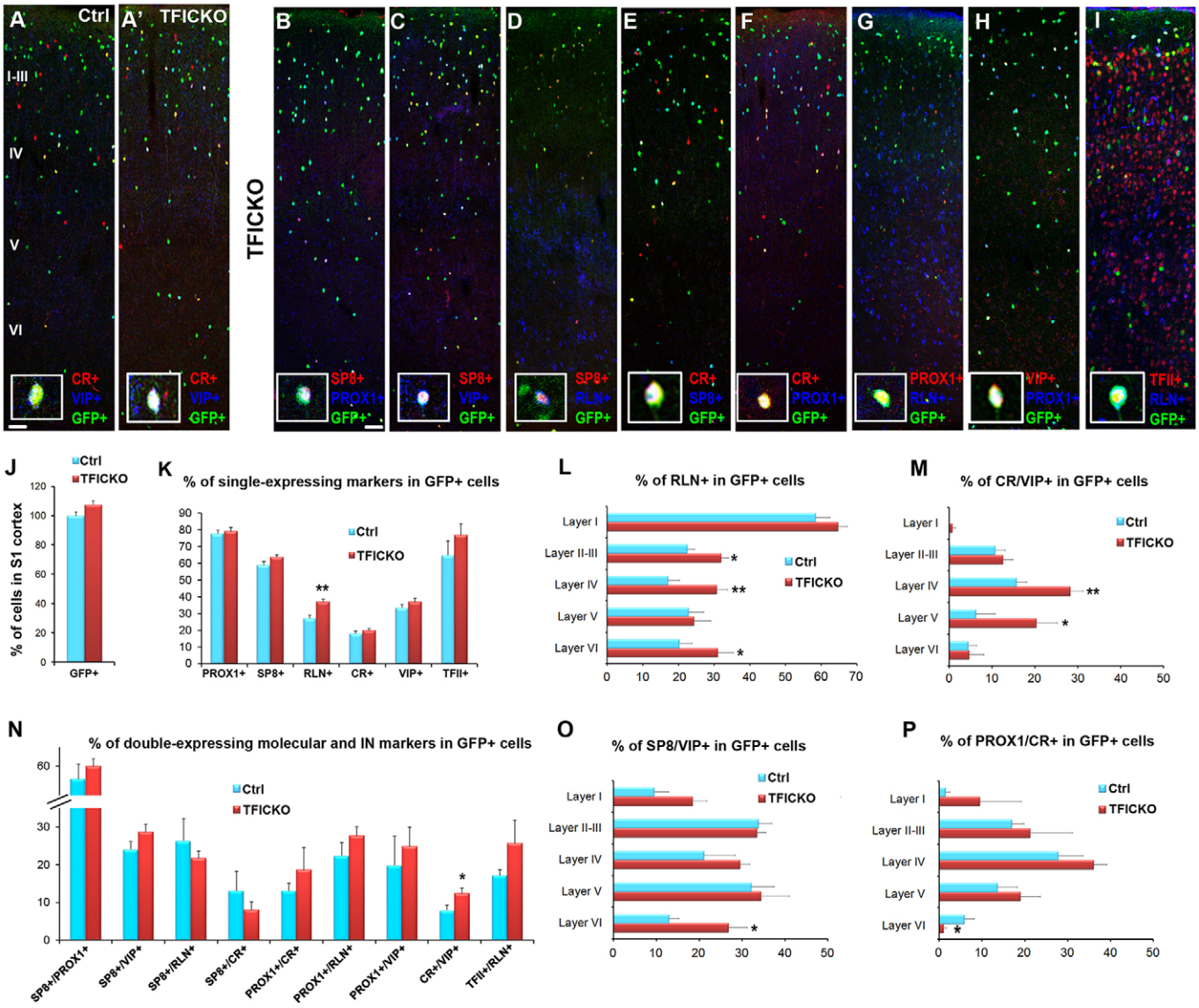

Fig. 8. Altered number and laminar distribution of IN subtypes in adult *5HT3aR-GFP*$^{+}$ *COUP-TFI* mutant brains. (A,A′) Coronal sections of 2-month-old control (Ctrl) and mutant (TFICKO) *5HT3aR-GFP*$^{+}$ somatosensory cortices (S1) expressing CR and VIP. (B-I) Coronal sections of TFICKO S1 immunostained with the antibodies indicated. Equivalent control sections are shown in Fig. 5C-J. Insets show representative triple-positive cells. (J) Histogram showing the percentage of GFP^{+} neurons in S1 of control and mutant brains relative to the number in controls (set at 100%). (K-M) Histograms illustrating the percentage of GFP^{+} cells expressing molecular or subtype-specific markers (K) and laminar distribution of RLN^{+} and double CR^{+}VIP^{+} INs (L,M) in adult control and mutant cortices. (N-P) Histograms depicting the percentage and laminar distribution of GFP^{+} cells double positive for molecular and IN markers in adult control and *COUP-TFI* CKO cortices. Data are represented as mean±s.e.m. *P≤0.05, **P≤0.01. Scale bars: 100 µm.

INs (Inta et al., 2008; Jiang et al., 2013; Li et al., 2011; Waclaw et al., 2006) and to a lesser extent to amygdala INs (Waclaw et al., 2010), double SP8^{+}PROX1^{+} cells in the LMS might be the main source of SP8^{+} cortical INs (Ma et al., 2012) (Fig. 9).

COUP-TFI controls the rostral but not the caudal migratory routes

Our data show that COUP-TF members are highly represented in all three streams. Interestingly, COUP-TFI controls the rate of CGE-migrating cells rostrally to the LGE and MGE, but not to the caudal pole. This is very different from COUP-TFII, which is crucial for driving CGE cells caudally (Kanatani et al., 2008, 2015). Thus, whereas COUP-TFI restricts the number of CGE cells migrating rostrally, COUP-TFII promotes CGE cells to take caudal directions. This suggests that COUP-TFI and COUP-TFII might have minor redundant functions in the CGE during the choice of migratory routes, possibly by controlling distinct guiding molecules and/or receptors. We also found that COUP-TFI acts on the LMS population expressing SP8 and on the MMS population expressing COUP-TFII. The regulation of COUP-TFI on *Sp8* expression has been well documented in the cortex (Alfano et al., 2014b; Borello et al., 2014), and control of COUP-TFI on *COUP-TFII* expression levels has been recently shown in the hippocampus (Flore et al., 2016). Thus, a similar mechanism in the CGE might limit the cohort of LMS SP8^{+} cells reaching the cortex, and compensate for the lack of COUP-TFI in the MMS, as previously proposed for the hippocampus, as both COUP-TFs have similar binding sites and could thus compete for the same target genes (Alfano et al., 2014a).

Our thorough analysis in adult COUP-TFI mutants has unravelled discrete differences in the CGE-derived GFP^{+} population of cortical

Development (2016) 143, 1753-1765 doi:10.1242/dev.131102

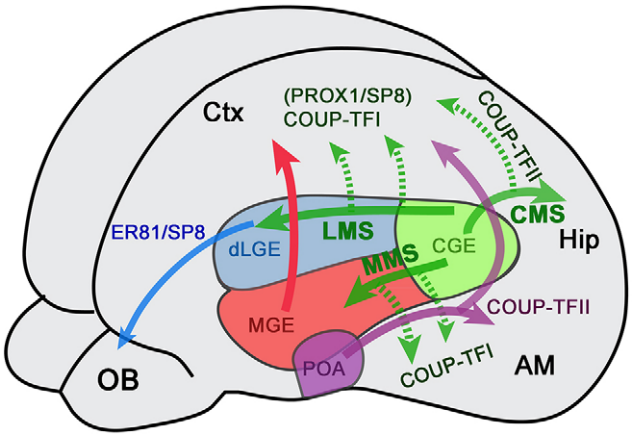

Fig. 9. Overview of the different subpallial migratory streams and their targets mentioned in this study. Schematic of the different migratory streams found in the subpallium. In green, the CGE-derived LMS and MMS described in this study, and the CMS described previously (Kanatani et al., 2008; Yozu et al., 2005). In red, the MGE-derived dorsal stream to the cortex (Ctx) reviewed by Guo and Anton (2014) and Marín (2013), and in magenta, the POA-derived ventral stream to the amygdala (AM) and cortex described previously (Hirata et al., 2009; Kanatani et al., 2015; Puelles et al., 2015). In blue, the dLGE-derived rostral stream migrating to the olfactory bulb (OB) and described by Batista-Brito et al. (2008) and Waclaw et al. (2006). Dashed arrows indicate putative migratory paths from LMS, MMS and CMS. Hip, hippocampus.

INs. In accordance with the increased embryological $SP8^+$ LMS population, we found more $SP8^+VIP^+$ cells in layer VI of the adult mutant somatosensory cortex. In the same layer, fewer $PROX1^+CR^+$ cells were detected, suggesting that COUP-TFI plays a particular function in CGE-derived cells of layer VI. This does not imply that COUP-TFI has no effect on other IN subtypes, as it limits the number of double CR^+VIP^+ cells in layers IV and V and RLN^+ INs in layers II-IV and VI. It is plausible that these changes might be mediated by altered PROX1 function because this factor plays a crucial role in the specification of these IN subtypes (Miyoshi et al., 2015), and/or by COUP-TFII highly expressed in the CR^+ populations (Varga et al., 2015; Reinchisi et al., 2012). We could not find any significant changes in the proportion of $PROX1^+VIP^+$, $PROX1^+CR^+$, $PROX1^+RLN^+$ or $COUP\text{-}TFII^+RLN^+$ INs in mutant brains even if their values tend to be increased. We hypothesize that the small amount of IN subtypes expressing GFP and a particular molecular marker can easily vary between samples, or, as in the case for COUP-TFII, compensatory mechanisms might act between embryological and adult stages. Together, our data show that COUP-TFI acts independently in distinct MGE- and CGE-derived IN subtypes to form a proper cortical inhibitory circuit and that in its absence mice become more resistant to GABA-dependent pharmacologically induced seizures (Lodato et al., 2011b).

Overall, this work reveals two novel migratory paths for CGE-derived INs in the mouse subpallium. These routes express a distinct combination of transcription factors and contribute to the laminar specification of individual subtypes in the neocortex and to specific amygdaloid nuclei. We thus propose that the existence of spatially and temporally regulated paths in the subpallium helps to direct the different IN populations towards their brain targets.

MATERIALS AND METHODS

Mice

The *5HT3aR-GFP* transgenic line was provided by the GENSAT consortium and conditional IN-specific *COUP-TFI* CKO mice were generated as previously reported (Lodato et al., 2011b) and propagated in a C57BL/6J (Charles River) inbred strain. We used $COUP\text{-}TFI^{flox/+}$, $COUP\text{-}TFI^{flox/flox}$ or *Dlx5/6-Cre*-positive (Cre^+) mice as controls, because they show no phenotypic abnormalities (Stenman et al., 2003; Armentano et al., 2007). We found no phenotypic differences between genders. Genotyping was performed as previously described (Lodato et al., 2011b). Timed pregnant embryos were obtained by overnight mating and the following morning was counted as E0.5. All experiments were conducted according to French ethical regulations and this project received the approval from our local ethics committee (CIEPAL NCE/2014-209).

Brain and embryo fixation

Mice were perfused with 4% buffered paraformaldehyde (PFA) and adult brains were post-fixed in 4% PFA for 12 h at 4°C. Decapitated heads of embryos (E11.5 to E18.5) were fixed in 4% PFA for 12 h at 4°C and then brains were post-fixed in 4% PFA for 2 h at 4°C.

Immunofluorescence

Vibratome sections were processed for free-floating immunofluorescence (IF), as previously described (Lodato et al., 2011b) with the following primary antibodies: anti-calbindin (rabbit, 1:500, Swant CB-38a); anti-calretinin (rabbit, 1:5000, Swant 7699/4); anti-calretinin (mouse, 1:500, Millipore MAB1568); anti-COUP-TFI (mouse, 1:100, Abcam ab41858); anti-COUP-TFII (rabbit, 1:500; Tripodi et al., 2004); anti-ER81 (rabbit, 1:2000, gift from Silvia Arber); anti-GFP (rabbit, 1:1000, Molecular Probes A11122); anti-GFP (chicken, 1:800, Abcam ab13970); anti-NKX2.1 (rabbit, 1:300, Santa Cruz sc13040); anti-PROX1 N terminus (goat, 1:700, R&D Systems AF2727); anti-PROX1 C terminus (rabbit, 1:1000, Abcam 11941-100); anti-RLN (mouse, 1:500, Millipore MAB5364); anti-SP8 (goat, 1:500, Santa Cruz sc104661); anti-TBR1 (rabbit, 1:500, Abcam ab31940) and anti-VIP (rabbit, 1:500, ImmunoStar 20077). The following secondary antibodies were used: Alexa Fluor 488-conjugated anti-chicken; Alexa Fluor 488-conjugated anti-rabbit; Alexa Fluor 488-conjugated anti-mouse; Alexa Fluor 594-conjugated anti-rabbit; Alexa Fluor 594-conjugated anti-mouse; Alexa Fluor 594-conjugated anti-goat; Alexa Fluor 594-conjugated anti-rat; Alexa Fluor 647-conjugated anti-rabbit; Alexa Fluor 647-conjugated anti-mouse; Alexa Fluor 647-conjugated anti-rat (Invitrogen; all 1:300). All experiments were repeated at least three times.

EdU birthdating

Timed pregnant females received a single intraperitoneal injection of 5-ethynyl-2′-deoxyuridine (EdU) (50 mg/kg) 1 h before sacrifice and embryos were collected at E13.5 and processed for EdU antibody staining according to the manufacturer's instructions (Click-iT EdU Imaging Kit C10340, Invitrogen). A set of three wild-type and *COUP-TFI* CKO embryos were examined for EdU^+ cell distribution in the CGE, and cells in the VZ and SVZ were separately counted.

Organotypic slice cultures

Brains were embedded in 3% low melting agarose and cut horizontally using a vibratome (Leica VT1000S) at 300 µm thickness. Slices were cultured for 2 or 4 days in Neurobasal Medium (Gibco) plus N-2 and B27 supplements (Gibco), as previously described (Tripodi et al., 2004). The Cell Tracker Red CMTPX (Molecular Probes C34552) was diluted to 1 mM and impregnated on resin beads (Bio-Rad 1401241). One bead or one DiI crystal was introduced in the CGE after 2 h of culture. After incubation, the bead was carefully removed and slices were fixed in 4% PFA for 4 h at 4°C and processed for IF, as indicated above. In co-culture experiments, the CGE explant from a GFP^+ embryo was transplanted into the CGE of a non-GFP^+ host littermate and incubated for 2 days, before analysis.

In utero cell transplantation

Homochronic transplantations were performed using E14/E14.5 donor and host embryos as previously described (Vucurovic et al., 2010). Three CGEs from E14/E14.5 *5HT3aR-GFP* donors were used to produce the cell suspension that was injected into the ventricles of host OF1 mice. The progeny was sacrificed at P21 and processed for IF, as described above. The distribution of $5HT3aR\text{-}GFP^+$ grafted cells was determined on coronal sections of three animals (947

Development (2016) 143, 1753-1765 doi:10.1242/dev.131102

GFP$^+$ cells) in the somatosensory cortex, the hippocampus and the amygdala. All the data of each structure were pooled together in order to estimate a representative distribution of GFP$^+$ cells in the brain.

Imaging

Sections were imaged using a Leica DM6000B microscope, a Leica SPE confocal microscope or a Zeiss 710 confocal microscope and images were acquired using LAS AF (Leica) or ZEN (Zeiss) software and processed with Adobe Photoshop and ImageJ software.

Cell counting

For quantification of IN subpopulations at embryonic stages, a representative area in the migratory paths was selected for each animal (n=3) and single- or double-positive cells were counted. For quantification of IN subpopulations in the adult, three coronal anatomically matched sections in the somatosensory cortex along the rostro-caudal axis were selected from littermate mice. Digital boxes of fixed width were superimposed on each coronal section and subdivided into ten sampling areas (bins) with a dorso-ventral extent from the pial surface to the white matter. Deep layers (VI-IV) were assigned to bin 1 to 7 and upper layers (III-I) were assigned to bin 8 to 10, based on anatomical features. All cell detections and counts were performed using Photoshop software.

Data analysis

Cell quantification data and graphs were constructed using Microsoft Excel software. For each genotype, a mean value was calculated from all counted sections. Error bars represent the standard error of the mean (s.e.m.). Statistical significance was determined using two-tailed Student's t-tests (*P<0.05, **P<0.01, ***P<0.001).

Acknowledgements

We thank K. Campbell for the *Dlx5/6-Cre* line; Silvia Arber for the ER81 antibody; Eya Setti and Nadia Elganfoud for their technical help; and the whole Studer lab for fruitful discussions.

Competing interests

The authors declare no competing or financial interests.

Author contributions

M.S. conceived and supervised the study, and wrote the manuscript. A.T. and N.R.-R. designed and performed experiments, interpreted the data and reviewed the manuscript. T.V. designed and performed the *in utero* graft experiment, and reviewed the manuscript.

Funding

This work was supported by the French National Research Agency (Agence Nationale de la Recherche; ANR) [ANR-13-BSV4-0011 to M.S.] and the French Government through the 'Investments for the Future' LABEX SIGNALIFE [ANR-11-LABX-0028-01 to M.S.]; a fellowship from the Fondation pour la Recherche Médicale (FRM) [FDT20130928192 to A.T.]; and an FPI fellowship from the Government of Spain (Ministerio de Economía y Competitividad) [BES-2011-043865 to N.R.-R.].

Supplementary information

Supplementary information available online at
http://dev.biologists.org/lookup/suppl/doi:10.1242/dev.131102/-/DC1

References

Alfano, C., Magrinelli, E., Harb, K. and Studer, M. (2014a). The nuclear receptors COUP-TF: a long-lasting experience in forebrain assembly. *Cell. Mol. Life Sci.* **71**, 43-62.

Alfano, C., Magrinelli, E., Harb, K., Hevner, R. F. and Studer, M. (2014b). Postmitotic control of sensory area specification during neocortical development. *Nat. Commun.* **5**, 5632.

Anderson, S. A., Marín, O., Horn, C., Jennings, K. and Rubenstein, J. L. (2001). Distinct cortical migrations from the medial and lateral ganglionic eminences. *Development* **128**, 353-363.

Armentano, M., Chou, S.-J., Srubek Tomassy, G., Leingärtner, A., O'Leary, D. D. and Studer, M. (2007). COUP-TFI regulates the balance of cortical patterning between frontal/motor and sensory areas. *Nat. Neurosci.* **10**, 1277-1286.

Batista-Brito, R., Close, J., Machold, R. and Fishell, G. (2008). The distinct temporal origins of olfactory bulb interneuron subtypes. *J. Neurosci.* **28**, 3966-3975.

Borello, U., Madhavan, M., Vilinsky, I., Faedo, A., Pierani, A., Rubenstein, J. and Campbell, K. (2014). Sp8 and COUP-TF1 reciprocally regulate patterning and Fgf signaling in cortical progenitors. *Cereb. Cortex* **24**, 1409-1421.

Butt, S. J. B., Fuccillo, M., Nery, S., Noctor, S., Kriegstein, A., Corbin, J. G. and Fishell, G. (2005). The temporal and spatial origins of cortical interneurons predict their physiological subtype. *Neuron* **48**, 591-604.

Cai, Y., Zhang, Q., Wang, C., Zhang, Y., Ma, T., Zhou, X., Tian, M., Rubenstein, J. L. R. and Yang, Z. (2013). Nuclear receptor COUP-TFII-expressing neocortical interneurons are derived from the medial and lateral/caudal ganglionic eminence and define specific subsets of mature interneurons. *J. Comp. Neurol.* **521**, 479-497.

Chameau, P., Inta, D., Vitalis, T., Monyer, H., Wadman, W. J. and van Hooft, J. A. (2009). The N-terminal region of reelin regulates postnatal dendritic maturation of cortical pyramidal neurons. *Proc. Natl. Acad. Sci. USA* **106**, 7227-7232.

Chittajallu, R., Craig, M. T., McFarland, A., Yuan, X., Gerfen, S., Tricoire, L., Erkkila, B., Barron, S. C., Lopez, C. M., Liang, B. J. et al. (2013). Dual origins of functionally distinct O-LM interneurons revealed by differential 5-HT(3A)R expression. *Nat. Neurosci.* **16**, 1598-1607.

Engel, M., Smidt, M. P. and van Hooft, J. A. (2013). The serotonin 5-HT3 receptor: a novel neurodevelopmental target. *Front. Cell. Neurosci.* **7**, 76.

Flore, G., Di Ruberto, G., Parisot, J., Sannino, S., Russo, F., Illingworth, E. A., Studer, M. and De Leonibus, E. (2016). Gradient COUP-TFI expression is required for functional organization of the hippocampal septo-temporal longitudinal axis. *Cereb. Cortex* pii: bhv336.

Fogarty, M., Grist, M., Gelman, D., Marín, O., Pachnis, V. and Kessaris, N. (2007). Spatial genetic patterning of the embryonic neuroepithelium generates GABAergic interneuron diversity in the adult cortex. *J. Neurosci.* **27**, 10935-10946.

Gelman, D. M., Martini, F. J., Nobrega-Pereira, S., Pierani, A., Kessaris, N. and Marin, O. (2009). The embryonic preoptic area is a novel source of cortical GABAergic interneurons. *J. Neurosci.* **29**, 9380-9389.

Gelman, D., Griveau, A., Dehorter, N., Teissier, A., Varela, C., Pla, R., Pierani, A. and Marin, O. (2011). A wide diversity of cortical GABAergic interneurons derives from the embryonic preoptic area. *J. Neurosci.* **31**, 16570-16580.

Guo, J. and Anton, E. S. (2014). Decision making during interneuron migration in the developing cerebral cortex. *Trends Cell Biol.* **24**, 342-351.

Haugland, R. (2002). *Handbook of Fluorescent Probes and Research Products*. New York: Molecular Probes, Inc.

Hevner, R. F., Shi, L., Justice, N., Hsueh, Y.-P., Sheng, M., Smiga, S., Bulfone, A., Goffinet, A. M., Campagnoni, A. T. and Rubenstein, J. L. R. (2001). Tbr1 regulates differentiation of the preplate and layer 6. *Neuron* **29**, 353-366.

Hirata, T., Li, P., Lanuza, G. M., Cocas, L. A., Huntsman, M. M. and Corbin, J. G. (2009). Identification of distinct telencephalic progenitor pools for neuronal diversity in the amygdala. *Nat. Neurosci.* **12**, 141-149.

Inta, D., Alfonso, J., von Engelhardt, J., Kreuzberg, M. M., Meyer, A. H., van Hooft, J. A. and Monyer, H. (2008). Neurogenesis and widespread forebrain migration of distinct GABAergic neurons from the postnatal subventricular zone. *Proc. Natl. Acad. Sci. USA* **105**, 20994-20999.

Jiang, X., Zhang, M., You, Y. and Liu, F. (2013). The production of somatostatin interneurons in the olfactory bulb is regulated by the transcription factor sp8. *PLoS ONE* **8**, e70049.

Jiménez, D., López-Mascaraque, L. M., Valverde, F. and De Carlos, J. A. (2002). Tangential migration in neocortical development. *Dev. Biol.* **244**, 155-169.

Kanatani, S., Yozu, M., Tabata, H. and Nakajima, K. (2008). COUP-TFII is preferentially expressed in the caudal ganglionic eminence and is involved in the caudal migratory stream. *J. Neurosci.* **28**, 13582-13591.

Kanatani, S., Honda, T., Aramaki, M., Hayashi, K., Kubo, K.-i., Ishida, M., Tanaka, D. H., Kawauchi, T., Sekine, K., Kusuzawa, S. et al. (2015). The COUP-TFII/Neuropilin-2 is a molecular switch steering diencephalon-derived GABAergic neurons in the developing mouse brain. *Proc. Natl. Acad. Sci. USA* **112**, E4985-E4994.

Kessaris, N., Magno, L., Rubin, A. N. and Oliveira, M. G. (2014). Genetic programs controlling cortical interneuron fate. *Curr. Opin. Neurobiol.* **26**, 79-87.

Lee, S., Hjerling-Leffler, J., Zagha, E., Fishell, G. and Rudy, B. (2010). The largest group of superficial neocortical GABAergic interneurons expresses ionotropic serotonin receptors. *J. Neurosci.* **30**, 16796-16808.

Li, X., Sun, C., Lin, C., Ma, T., Madhavan, M. C., Campbell, K. and Yang, Z. (2011). The transcription factor Sp8 is required for the production of parvalbumin-expressing interneurons in the olfactory bulb. *J. Neurosci.* **31**, 8450-8455.

Lodato, S., Rouaux, C., Quast, K. B., Jantrachotechatchawan, C., Studer, M., Hensch, T. K. and Arlotta, P. (2011a). Excitatory projection neuron subtypes control the distribution of local inhibitory interneurons in the cerebral cortex. *Neuron* **69**, 763-779.

Lodato, S., Tomassy, G. S., De Leonibus, E., Uzcategui, Y. G., Andolfi, G., Armentano, M., Touzot, A., Gaztelu, J. M., Arlotta, P., Menendez de la Prida, L. et al. (2011b). Loss of COUP-TFI alters the balance between caudal ganglionic eminence- and medial ganglionic eminence-derived cortical interneurons and results in resistance to epilepsy. *J. Neurosci.* **31**, 4650-4662.

Ma, T., Zhang, Q., Cai, Y., You, Y., Rubenstein, J. L. R. and Yang, Z. (2012). A subpopulation of dorsal lateral/caudal ganglionic eminence-derived neocortical

interneurons expresses the transcription factor Sp8. *Cereb. Cortex* **22**, 2120-2130.
Marín, O. (2013). Cellular and molecular mechanisms controlling the migration of neocortical interneurons. *Eur. J. Neurosci.* **38**, 2019-2029.
Miyoshi, G. and Fishell, G. (2011). GABAergic interneuron lineages selectively sort into specific cortical layers during early postnatal development. *Cereb. Cortex* **21**, 845-852.
Miyoshi, G., Butt, S. J. B., Takebayashi, H. and Fishell, G. (2007). Physiologically distinct temporal cohorts of cortical interneurons arise from telencephalic Olig2-expressing precursors. *J. Neurosci.* **27**, 7786-7798.
Miyoshi, G., Hjerling-Leffler, J., Karayannis, T., Sousa, V. H., Butt, S. J. B., Battiste, J., Johnson, J. E., Machold, R. P. and Fishell, G. (2010). Genetic fate mapping reveals that the caudal ganglionic eminence produces a large and diverse population of superficial cortical interneurons. *J. Neurosci.* **30**, 1582-1594.
Miyoshi, G., Young, A., Petros, T., Karayannis, T., McKenzie Chang, M., Lavado, A., Iwano, T., Nakajima, M., Taniguchi, H., Huang, Z. J. et al. (2015). Prox1 regulates the subtype-specific development of caudal ganglionic eminence-derived GABAergic cortical interneurons. *J. Neurosci.* **35**, 12869-12889.
Murthy, S., Niquille, M., Hurni, N., Limoni, G., Frazer, S., Chameau, P., van Hooft, J. A., Vitalis, T. and Dayer, A. (2014). Serotonin receptor 3A controls interneuron migration into the neocortex. *Nat. Commun.* **5**, 5524.
Nery, S., Fishell, G. and Corbin, J. G. (2002). The caudal ganglionic eminence is a source of distinct cortical and subcortical cell populations. *Nat. Neurosci.* **5**, 1279-1287.
Puelles, L., Morales-Delgado, N., Merchán, P., Castro-Robles, B., Martínez-de-la-Torre, M., Díaz, C. and Ferran, J. L. (2015). Radial and tangential migration of telencephalic somatostatin neurons originated from the mouse diagonal area. *Brain Struct. Funct.* 1-39.
Reinchisi, G., Ijichi, K., Glidden, N., Jakovcevski, I. and Zecevic, N. (2012). COUP-TFII expressing interneurons in human fetal forebrain. *Cereb. Cortex* **22**, 2820-2830.
Rubin, A. N. and Kessaris, N. (2013). PROX1: a lineage tracer for cortical interneurons originating in the lateral/caudal ganglionic eminence and preoptic area. *PLoS ONE* **8**, e77339.
Rudy, B., Fishell, G., Lee, S. and Hjerling-Leffler, J. (2011). Three groups of interneurons account for nearly 100% of neocortical GABAergic neurons. *Dev. Neurobiol.* **71**, 45-61.
Stenman, J., Toresson, H. and Campbell, K. (2003). Identification of two distinct progenitor populations in the lateral ganglionic eminence: implications for striatal and olfactory bulb neurogenesis. *J. Neurosci.* **23**, 167-174.
Sussel, L., Marin, O., Kimura, S. and Rubenstein, J. L. (1999). Loss of Nkx2.1 homeobox gene function results in a ventral to dorsal molecular respecification within the basal telencephalon: evidence for a transformation of the pallidum into the striatum. *Development* **126**, 3359-3370.
Tanaka, D. H. and Nakajima, K. (2012). Migratory pathways of GABAergic interneurons when they enter the neocortex. *Eur. J. Neurosci.* **35**, 1655-1660.
Tang, K., Rubenstein, J. L. R., Tsai, S. Y. and Tsai, M.-J. (2012). COUP-TFII controls amygdala patterning by regulating neuropilin expression. *Development* **139**, 1630-1639.
Tripodi, M., Filosa, A., Armentano, M. and Studer, M. (2004). The COUP-TF nuclear receptors regulate cell migration in the mammalian basal forebrain. *Development* **131**, 6119-6129.
Valcanis, H. and Tan, S.-S. S. (2003). Layer specification of transplanted interneurons in developing mouse neocortex. *J. Neurosci.* **23**, 5113-5122.
Varga, C., Tamas, G., Barzo, P., Olah, S. and Somogyi, P. (2015). Molecular and electrophysiological characterization of GABAergic interneurons expressing the transcription factor COUP-TFII in the adult human temporal cortex. *Cereb. Cortex* **25**, 4430-4449.
Vitalis, T. and Rossier, J. (2011). New insights into cortical interneurons development and classification: contribution of developmental studies. *Dev. Neurobiol.* **71**, 34-44.
Vucurovic, K., Gallopin, T., Ferezou, I., Rancillac, A., Chameau, P., van Hooft, J. A., Geoffroy, H., Monyer, H., Rossier, J. and Vitalis, T. (2010). Serotonin 3A receptor subtype as an early and protracted marker of cortical interneuron subpopulations. *Cereb. Cortex* **20**, 2333-2347.
Waclaw, R. R., Allen, Z. J., II, Bell, S. M., Erdélyi, F., Szabó, G., Potter, S. S. and Campbell, K. (2006). The zinc finger transcription factor Sp8 regulates the generation and diversity of olfactory bulb interneurons. *Neuron* **49**, 503-516.
Waclaw, R. R., Ehrman, L. A., Pierani, A. and Campbell, K. (2010). Developmental origin of the neuronal subtypes that comprise the amygdalar fear circuit in the mouse. *J. Neurosci.* **30**, 6944-6953.
Wichterle, H., Turnbull, D. H., Nery, S., Fishell, G. and Alvarez-Buylla, A. (2001). In utero fate mapping reveals distinct migratory pathways and fates of neurons born in the mammalian basal forebrain. *Development* **128**, 3759-3771.
Xu, Q., Cobos, I., De La Cruz, E., Rubenstein, J. L. and Anderson, S. A. (2004). Origins of cortical interneuron subtypes. *J. Neurosci.* **24**, 2612-2622.
Xu, Q., Tam, M. and Anderson, S. A. (2008). Fate mapping Nkx2.1-lineage cells in the mouse telencephalon. *J. Comp. Neurol.* **506**, 16-29.
Yozu, M., Tabata, H. and Nakajima, K. (2005). The caudal migratory stream: a novel migratory stream of interneurons derived from the caudal ganglionic eminence in the developing mouse forebrain. *J. Neurosci.* **25**, 7268-7277.

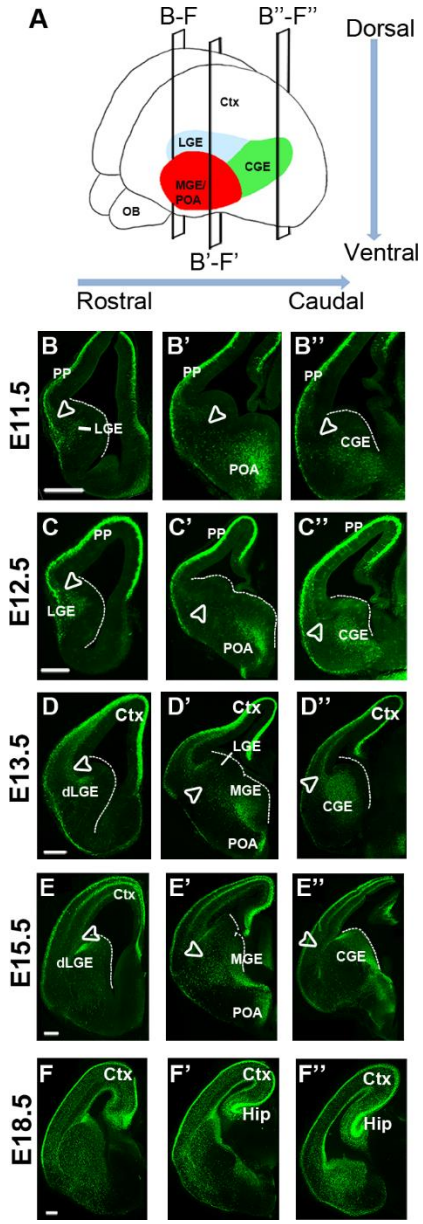

Fig. S1. Anterior to posterior views of the different 5HT3aR-GFP+ migratory streams in the developing mouse. (**A**) Schematic of a mouse brain indicating the position of coronal sections illustrated in B to F''. (**B-F''**) Rostral to caudal sequential coronal sections of *5HT3aR-GFP* embryos immunostained with GFP at the stages indicated on the left. *Empty arrowheads* point to dorsally-migrating GFP+ cells. *Abbreviations: LGE, lateral ganglionic eminence; dLGE, dorsal lateral ganglionic eminence; MGE, medial ganglionic eminence; CGE, caudal ganglionic eminence; POA, preoptic area; PP, preplate; Ctx, cortex; Hip, hippocampus. Scale bars: 300µm.*

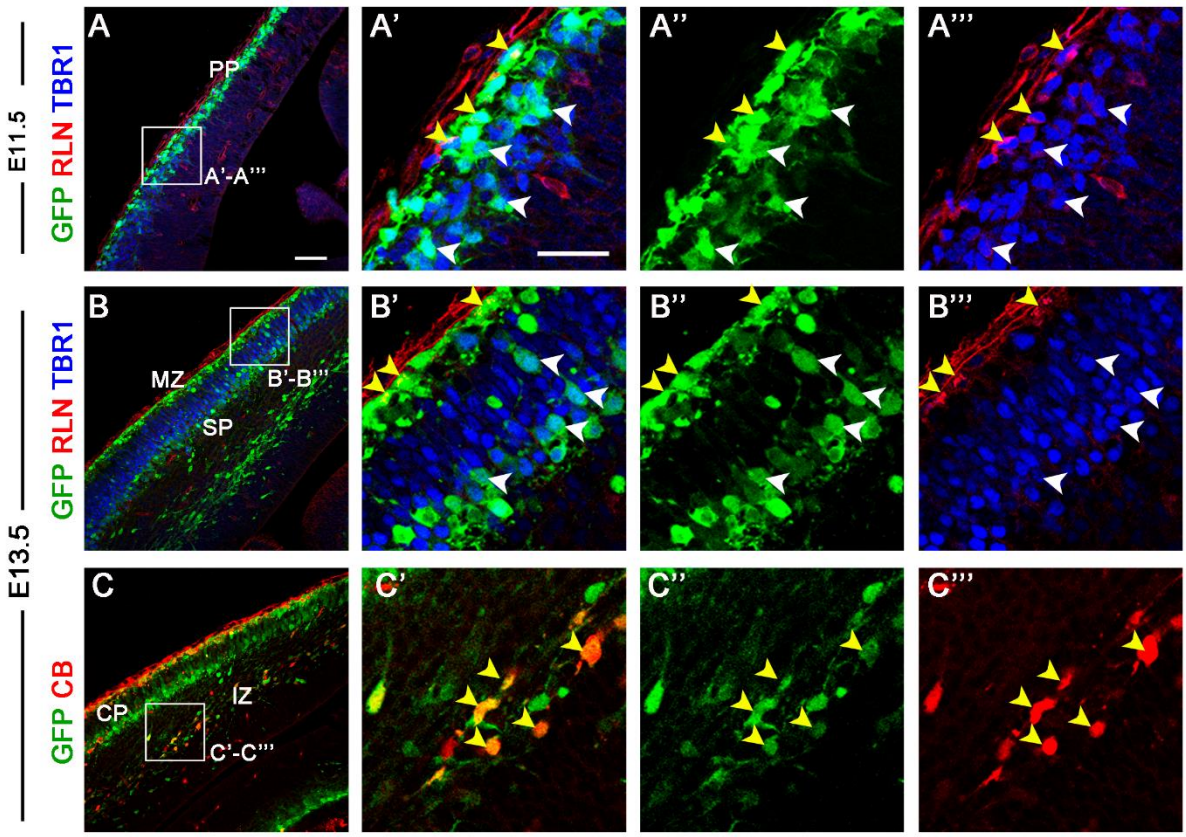

Fig. S2. Expression of 5HT3aR-GFP in preplate cells at early stages of development. (A, B) Coronal sections of E11.5 and E13.5 *5HT3aR-GFP* embryos immunostained with GFP, RLN and TBR1. At E11.5, GFP is expressed in Cajal-Retzius cells in the upper preplate (PP) (yellow arrowheads in **A'-A'''**) and in early pioneer cortical neurons in the PP (white arrowheads in **A'-A'''**). At E13.5, Cajal-Retzius cells remain in the marginal zone (MZ) (yellow arrowheads in **B'-B'''**), whereas the TBR1/GFP + cells are localized in the subplate (SP) (white arrowheads in **B'-B'''**). **(C-C''')** Coronal section of E13.5 *5HT3aR-GFP* embryos immunostained with GFP and Calbindin (CB). CB/GFP + cells are found in the MZ and intermediate zone (IZ) of the cortex corresponding to migratory interneurons (yellow arrowheads). *Abbreviations; PP, preplate; MZ, marginal zone; SP, subplate; CP, cortical plate; IZ, intermediate zone. Scale bars: (A) 50 µm, (A') 25 µm.*

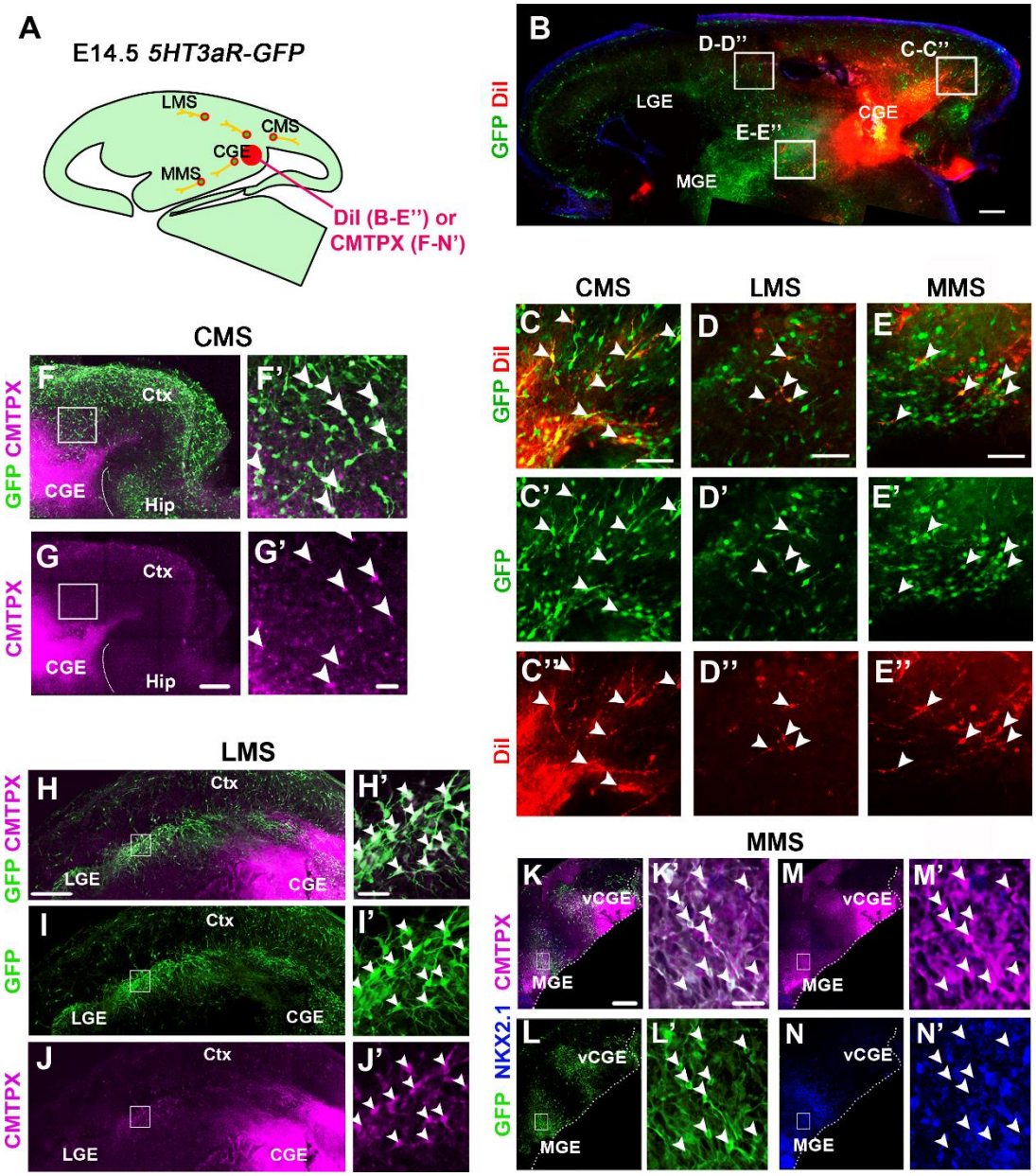

Fig. S3. Further experimental validation of rostrally and caudally CGE-derived *5HT3aR-GFP*+ migration. (**A**) Schematic of the experimental approach illustrating the positions of the resin ball soaked with CMTPX or DiI in the CGE of E14.5 horizontal organotypic sections. (**B**) Whole view of a horizontal *5HT3aR-GFP*+ section injected with DiI after 2 DIV of culture. Boxes indicate the region highlighted in C-E''. (**C-E''**) High magnification views of the boxes shown above indicate (white arrowheads) the cells that have integrated the DiI and express GFP. Note that these cells are present in all three streams. (**F-G'**) Caudal views showing the localization of the cell tracker CMTPX in the CGE and in migrating cells (**G, G'** in magenta) and its co-localization with GFP (**F, F'** GFP in green) in the caudal migratory stream (CMS). (**H-J'**) Dorsal views illustrating the localization of the cell tracker CMTPX, the GFP staining and their co-localization in the lateral migratory stream (LMS). (**K-N'**) Ventral views depicting the localization of the cell tracker CMTPX, the GFP and the MGE marker NKX2.1. Cells co-expressing the CMTPX and GFP in the medial migratory stream (MMS) become white (arrowheads in K') and do not express NKX2.1 (in blue, N'). To the right, high magnification views of the boxes depicted to the left. Note that the intensity of the CMTPX staining in the CGE region has been highly enhanced so that single-traced cells are highlighted. *Abbreviations*: *LGE, lateral ganglionic eminence; MGE, medial ganglionic eminence; CGE, caudal ganglionic eminence; Ctx, cortex; Hip, hippocampus. Scale bars: (B,F-N) 300µm, (C-E'', F'-N'), 50µm.*

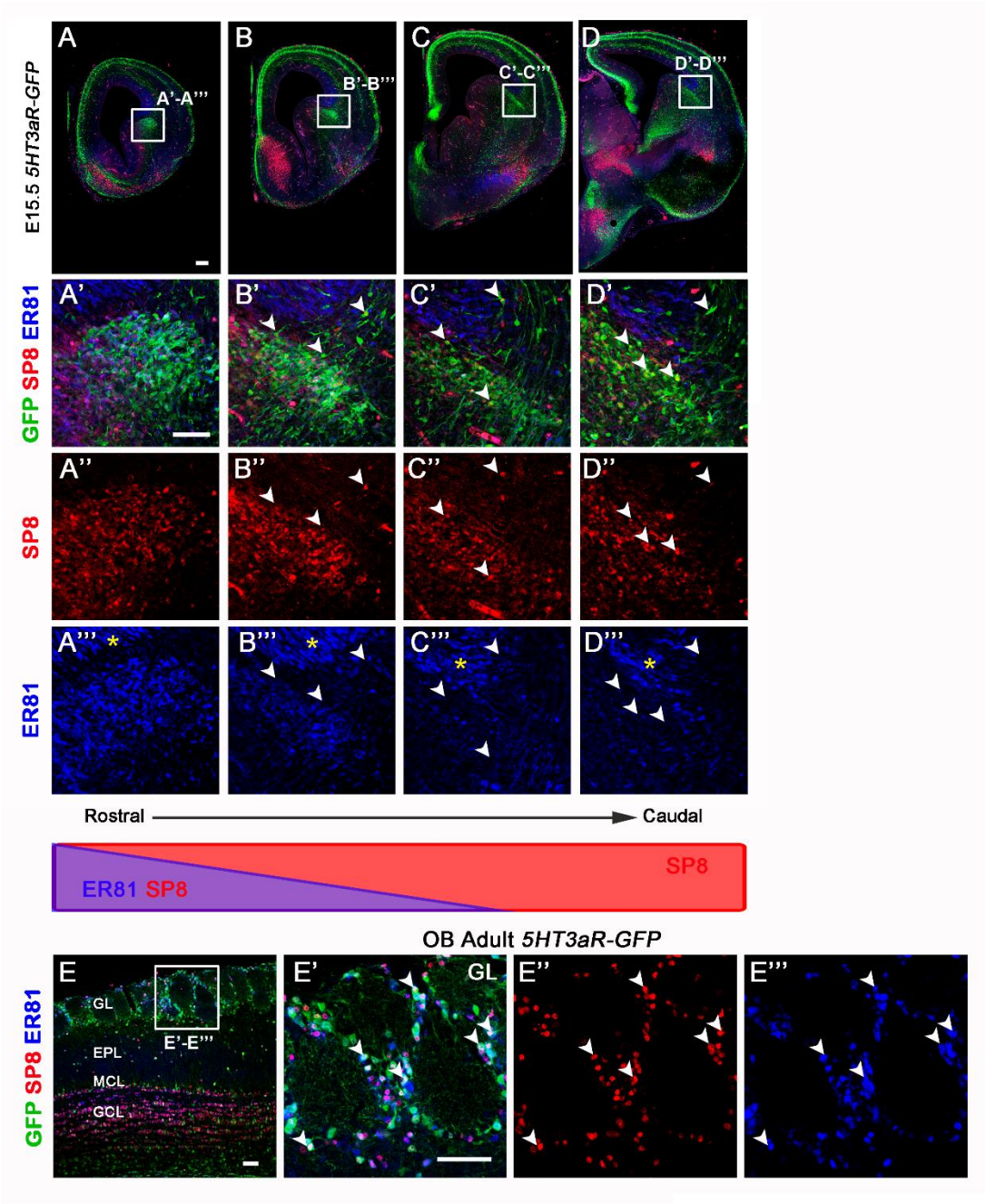

Fig. S4. ER81 is expressed in the rostral dLGE during development and in OB interneurons in adult mice. (**A-D**) Coronal sections of E15.5 *5HT3aR-GFP* embryos at four different rostrocaudal levels. The sections were immunostaining for GFP, SP8 and ER81. (**A'-D'''**) High magnification views taken from the boxes depicted in A-D. GFP and SP8 are expressed in the whole dLGE and in some neurons migrating through the intermediate zone to the cortex (white arrowheads in B'-D"). ER81 is expressed in the dLGE only at rostral levels and in the ventricular zone of the ventral pallium (yellow asterisks in A'''-D'''). Note that ER81 expression decreases from medial to caudal levels of the LGE and CGE. The arrowheads in B''' to D''' indicate double $GFP^{+}SP8^{+}$ cells and negative for ER81, migrating from the LMS to the cortex. (**E**) Coronal section of the olfactory bulb (OB) of adult *5HT3aR-GFP* mice showing the expression of GFP, SP8 and ER81 in different layers of the OB. (**E'-E'''**) High magnification views taken from the boxed area in (E) showing the expression of GFP, SP8 and ER81 in the glomerular layer (GL) of the OB. The majority of the GFP+ interneurons in the GL are positive for SP8 and ER81 (white arrowheads). *Abbreviations: GL, glomerular layer; EPL, external plexiform layer; MCL, mitral cell layer; GCL, granular cell layer. Scale bars: (A-D, E-E''') 100µm, (A'-D'''), 50µm.*

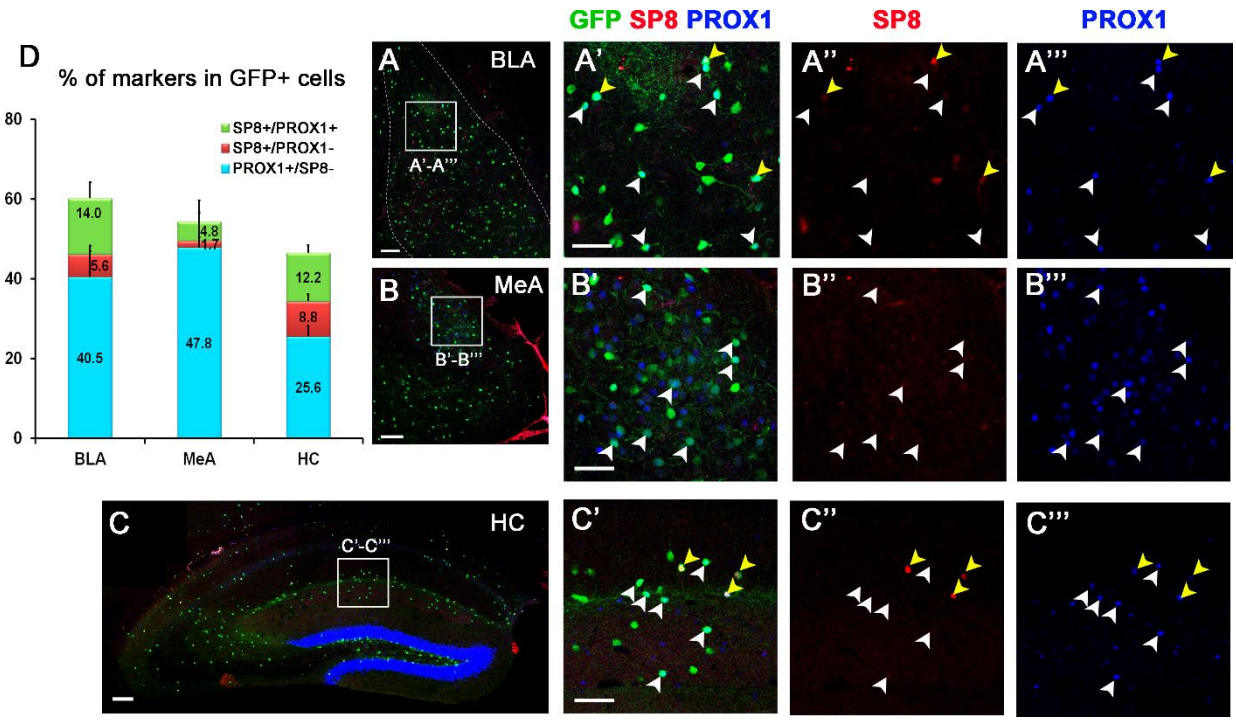

Fig. S5. GFP interneurons express SP8 and PROX1 in the amygdala and the hippocampus. (**A-C**) Coronal sections of adult *5HT3aR-GFP* mice in the basolateral complex of the amygdala (BLA), the medial amygdala (MeA) and the hippocampus (HC). The sections were immunostained for GFP, SP8 and PROX1. (**A'-C'''**) High magnification views taken from the boxed areas in A-C. The majority of GFP+ cells is positive for PROX1(white arrowheads), while a minor number of GFP+ cells is positive for SP8 (yellow arrowheads). (**D**) Graph showing the percentage of co-expression with PROX1and SP8 in the GFP+ population. In the amygdala, almost half of the GFP+ cells are positive for the transcription factor PROX1 and very few are positive only for SP8. *Scale bars: (A, B, C) 100µm, (A'-C''') 50µm.*